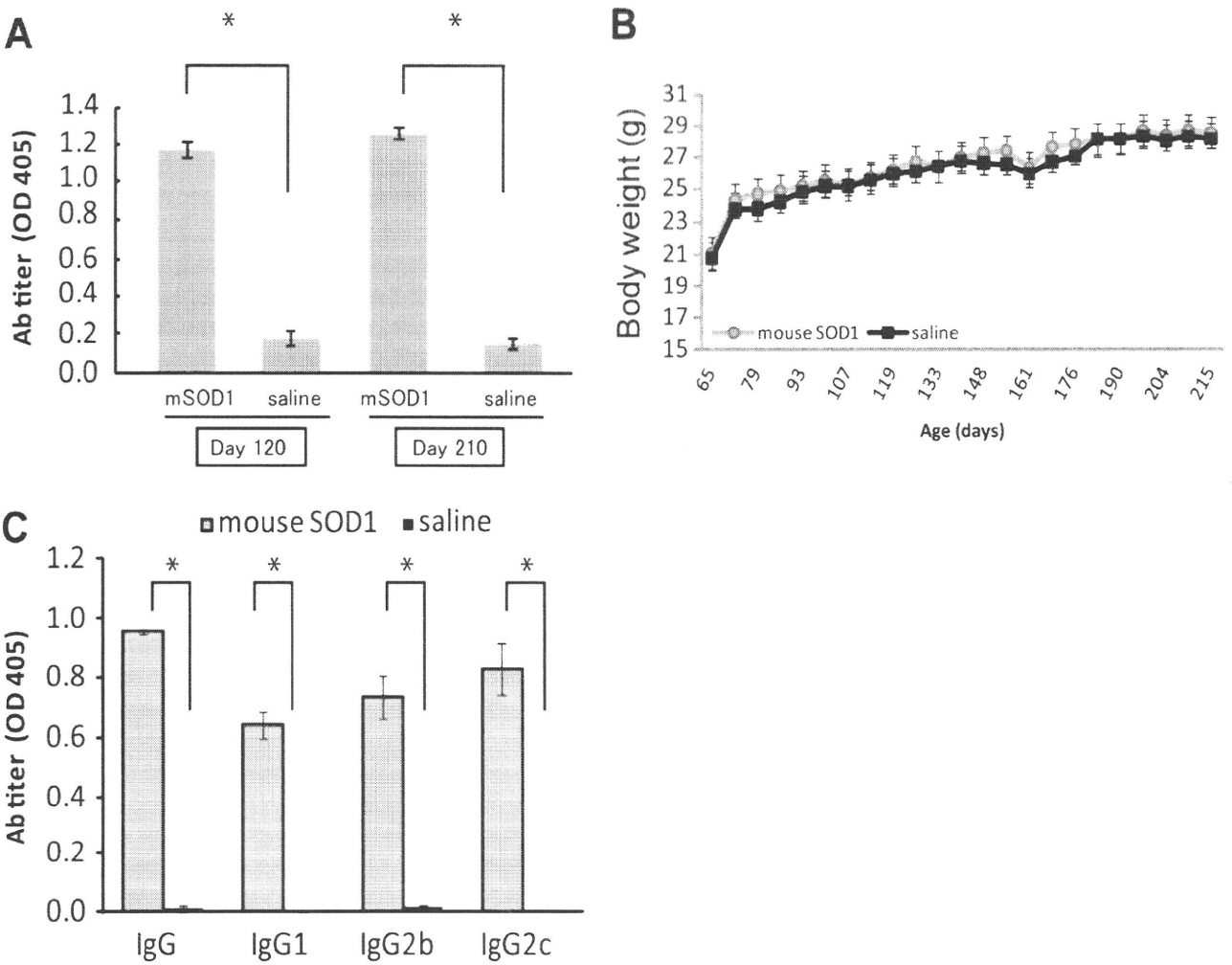

FIGURE 7. Vaccination of nontransgenic (non-Tg) mice using recombinant wild-type (WT) superoxide dismutase 1 (SOD1) protein effectively induces antibody with no detectable detrimental effect. **(A)** ELISA of sera of non-Tg mice vaccinated with mouse SOD1 and saline with adjuvant at days 120 and 210 (n = 5 in each group). Data show mean ± SEM (n = 5). *$p < 0.01$ by 1-way analysis of variance of Bonferroni test. **(B)** Comparison of body weights after vaccination between mouse SOD1-vaccinated and saline/adjuvant-injected controls. Each point shows mean body weight (g) of 5 mice per group. **(C)** ELISA for IgG subclasses induced by mouse SOD1 vaccination. The titer for IgG1, 2b, and 2c against recombinant mouse SOD1 was determined in sera from SOD1-vaccinated and control saline/adjuvant-injected mice at day 210 and expressed as OD 405 nm (mean ± SE forSE for each group, n = 5). *$p < 0.01$ by 1-way analysis of variance of Bonferroni test.

$r = 0.7333$, $p = 0.0156$, by Spearman r), whereas IgG1 and IgG2c showed no significant correlation (Figure, part B, a, c, Supplemental Digital Content 3, http://links.lww.com/NEN/A180). By contrast, there was no positive correlation of the G93A vaccination with any IgG subtype. Rather, the IgG1 titer was negatively correlated to the survival effect (Figure, part B, d, Supplemental Digital Content 3, http://links.lww.com/NEN/A180; $r = -0.5879$, $p = 0.0403$, by Spearman r).

Antibody Induction in Non-Tg Mice by Vaccination With Murine WT SOD1

Because the human WT SOD1 is a foreign antigen to mice, antibody is generally easily induced. For human trials, induction of the antibody against human WT-SOD1 in human body would be required. Therefore, we investigated whether the murine WT-apo SOD1 induced antibody by breaking immunologic tolerance to endogenous SOD1 in mice. Vaccination of non-Tg C57BL/6 mice with recombinant mouse WT-apo SOD1 induced antibody against mouse SOD1 at days 120 and 210 (Fig. 7A). Simultaneously, the adverse reactions of the vaccination were monitored for BW loss (Fig. 7B), movement, hair length, spontaneous activity, and provoked biting as well as observation of tissue hemorrhage or anemia at autopsy. These analyses displayed no abnormalities that could be attributed to vaccination. The analysis of IgG subclass profile showed that all the subclasses including IgG1, IgG2b, and IgG 2c were comparably elevated (Fig. 7C), indicating that both T_H1 and T_H2 immunity is induced in non-Tg mice.

DISCUSSION

In this report, we demonstrate a beneficial effect of vaccination with the WT-apo SOD1 protein to prolong the life

span of G93A SOD1 Tg mice. The chief effect was delaying the disease onset rather than slowing its progression. The G93A SOD1 vaccine also delayed the onset significantly and showed a trend to prolonging the life span. This result is in agreement with our previous finding that the vaccination with the G93A-apo SOD1 protein against G37R SOD1 mice (5 times higher) led to a 3-week delay of onset and a 4-week prolongation of life span, whereas the same vaccination of high-copy G93A SOD1 (G93AGur) mice (17 times higher) was not effective (10). Therefore, the expression level of the mutant protein in the Tg mice may determine the vaccine effect, particularly in the late stage. Because there generally are 1 or 2 copies of the mutant SOD1 gene in ALS patients, our results indicate that further development of vaccination aiming not only for prevention but also for disease inhibition after onset is warranted.

Unexpectedly, the apo-form of the SOD1 was a dimer, although the precise molecular features of the WT-apo SOD1 are unclear. The apo-SOD1 of both WT and G93A are slightly larger molecules than the holo-SOD1s, indicating that the apo-form of SOD1s form nonnative dimers. Intriguingly, the previous report showed that a nonnative SOD1 dimer is a common finding in mutant and sporadic ALS (24). Therefore, the misfolded dimeric conformation might mediate the vaccine effect of the WT-apo SOD1. Because of its utility regardless of the mutation type, the protective effect of the WT-apo SOD1 in G93AGur^{d1} mice may represent a widely applicable paradigm. We observed no detrimental effect of WT-apo SOD1 vaccination in G37R Tg mice, but there seemed to be some beneficial effect (personal observation). We and others have reported potential misfolding property of the WT SOD1 when posttranslationally modified such as monomerization (21) or oxidation (34), which may account for the effect of the WT-apo SOD1 vaccination. Therefore, further modification by narrowing the critical domains for misfolding or by specifying more aberrant structures such as oligomer or aggregates is a potential strategy for developing vaccines against mutant SOD1-linked ALS.

The precise mechanisms of the beneficial effects of vaccination with the misfolded SOD1 protein are unclear. We found that C1q increased around the remaining motor neurons and that IgG immunoreactivity increased in the spinal cord meninges. Moreover, the blood-brain barrier of mutant SOD1 Tg mice is fragile (35), and recent studies show $CD4^+$ T-cell proliferation in the spinal cord of mutant SOD1 Tg mice (17, 18). Therefore, it is conceivable that immune-related molecules or cells may easily penetrate into the CNS in mutant SOD1-linked ALS patients and that vaccine-induced antibodies could directly target extracellular SOD1 in the spinal cord. Although immunohistochemistry showed no obvious change in the SOD1 aggregates by the vaccination (not shown), this indicates that only small fractions of soluble misfolded species might participate in the extracellular toxicity.

Our results indicate that there is induction of protective immunity by vaccination with the Ribi adjuvant. The effect of both SOD1 vaccinations on T_H2 deviation in the spinal cord is striking. Moreover, STAT4 analysis suggests that activated microglia in the spinal cord of mutant SOD1 Tg mice are the source of IFNγ. Indeed, a recent report also showed that STAT4 is chiefly expressed in the active microglia in the cerebral white matter in multiple sclerosis (36). Active microglia expressing Mac-2 in the spinal cords are detected in presymptomatic mutant SOD1 Tg mice but not in non-Tg or WT SOD1 Tg mice (personal observation). Thus, microglia-derived IFNγ might be a pathogenic proinflammatory factor in mutant SOD1-linked ALS. Indeed, accumulating evidence also indicates the detrimental effect of IFNγ in the CNS, including oxidative stress (14), mitochondrial damage (30), and MHC class II+ cell proliferation (18). On the other hand, it should be noted that the toxicity of IFNγ is context-dependent and that it is regulated by a complex crosstalk between microglia and T-cell subtypes (37). It was reported that the stimulation of microglial cells with IFNγ rescues cells with various toxic challenges through the induction of IGF-1 (38) or IGF-2 (39). A recent study also shows that a low dose of IFNγ provides neuroprotection by enhancing neurogenesis in the amyloid precursor protein Tg mice (40). Therefore, the effects of IFNγ in the CNS are complex, and synergistic effects of other proinflammatory cytokines (e.g. TNF) in specific conditions likely are involved. Interestingly, the saline/adjuvant injection also promoted T_H2 deviation, possibly as a result of using the Ribi adjuvant (29). This result indicates that the adjuvant is crucial to acquire desirable effect of the vaccination, especially in ALS mutant mice. However, because of the lack of a therapeutic effect of saline/adjuvant injection, T_H2 deviation is not the primary mediator of the beneficial effects of vaccination.

We previously reported that late-stage G37R Tg mice with SOD1 vaccination had greater Mac2+ microglia than control mice (10). However, in the present study, analysis of the mice at the same point showed no significant difference in the number of Mac2+ microglia. Therefore, it may be that longer-lived mice with SOD1 vaccination showed more abundant microgliosis. Further analyses including in situ hybridization are needed to clarify this issue because of the diverse and complicated functions of microglia.

We show here that the both SOD1 vaccinations increased IL-4 mRNA levels in the spleen at an early time point and that there was a significant difference in IgG2c titer and IgG1/IgG2c ratio between the WT-apo and the G93A-apo vaccinations at the late stage. These results suggest that peripheral IL-4 may drive a T_H2 milieu from the early presymptomatic stage in the spinal cord, and circulating IFNγ may have some detrimental effect in the later period. Thus, the amount of IFNγ or TNF in the serum at the preclinical stage might be a useful marker for selecting an appropriate vaccine and adjuvant. Furthermore, the titer of each IgG subclass was not positively correlated in G93A-apo vaccination; rather, IgG1 titer was negatively correlated to the life span (Figure, Supplemental Digital Content, part B, d, http://links.lww.com/NEN/A180). These results suggest that T_H1/T_H2 regulation is unbalanced by the G93A vaccination in the Tg mice with the same mutation. Taken together, T_H1 deviation in the G93A vaccination in the later stage might counteract the effect to slow the progression. A recent report shows that IFNγ is increased in the serum of ALS patients (41). Moreover, systemically injected IFNγ distributes in the

brain (42) and it is known to disturb the immunologic privilege by the induction of MHC class I antigen in CNS cells (43). On the other hand, ablation of $CD4^+$ cells in mutant SOD1 Tg mice accelerated the ALS phenotype, which is mediated by microglial inhibition of IGF-1 (17). It was also reported that intravenous injection of regulatory or effecter T-cells significantly prolongs the longevity of G93A Tg mice (19). In a spinal cord injury model, externally injected macrophages potentiated the repair of damaged tissue by halting microglial activation (44). In such cases, anti-inflammatory cytokines including IL-4 (17) and IL-10 (45) mediate transfer of protective signals to microglia. Because there is potentially aberrant immunity in ALS, vaccinations should be cautiously designed. Considering recent conflicting reports as for therapeutic outcomes of a glatiramer acetate vaccination (46–49), in which an adjuvant is used only in the successful case (49) but not in other failures (46–48), it is possible that the repetitive challenges of a neuroprotective antigen without adjuvant may not suffice to evoke protective immunity. Therefore, in light of current understanding of the role of the inflammation in neurodegeneration, T_H1 /T_H2 balance may determine a detrimental/protective direction of neurons by regulating microglial function (50). Thus, it is important to recognize that a proper combination of antigen and adjuvant may synergistically augment the therapeutic effect of vaccination. Notably, the positive correlation between IgG2b (a subclass induced by TGFβ) and the therapeutic effect, including delay of disease onset and prolongation of the life span, prompts us to consider the benefit of mucosal immunity such as nasal or intestinal vaccination in which neuroprotective cytokines such as TGFβ and IL-4 are induced (51).

Vaccination of non-Tg mice with mouse WT SOD1 effectively induced antibody but did no overt harm. This is very important for the future application of anti-SOD1 antibody in terms of potential adverse reactions and immunologic tolerance. Abundant IgG2c as well as IgG1 was induced by the vaccination indicating that T_H1 immunity is provoked. Therefore, further modifications for the improvement of the vaccine effect include the development of misfolding structure–targeted vaccines, such as an oligomer or more narrowed sequences involved in the pathogenesis, the choice of adjuvant, and the route of vaccination.

In conclusion, our results indicate that WT-apo SOD1 may be a candidate as a vaccine for familial ALS patients with SOD1 mutations. Moreover, they suggest that induction of protective immunity and immunomodulation to suppress T_H1 immunity, particularly at the later stage, may enhance the outcome. Despite the advantage of passive immunization, which can abolish such immune response considerably, further improvement of vaccines will prove beneficial to familial ALS patients because of their long-lasting effects and of potential noninvasive ways for overcoming adverse reactions.

ACKNOWLEDGMENTS

The authors thank H. Kita and S. Nakamura for the technical assistance. The authors also thank Central Research Laboratory of Shiga University of Medical Science for experimental support. The authors are grateful to Ube Industries Ltd for kindly providing the recombinant human SOD1, chemically modified with 2-mercaptoethanol (2-ME-SOD1).

REFERENCES

1. Dion PA, Daoud H, Rouleau GA. Genetics of motor neuron disorders: New insights into pathogenic mechanisms. Nat Rev Genet 2009;10:769–82
2. Rosen DR, Siddique T, Patterson D, et al. Mutations in Cu/Zn superoxide dismutase gene are associated with familial amyotrophic lateral sclerosis. Nature 1993;362:59–62
3. Gurney ME, Pu H, Chiu AY, et al. Motor neuron degeneration in mice that express a human Cu,Zn superoxide dismutase mutation. Science 1994;264:1772–75
4. Clement AM, Nguyen MD, Roberts EA, et al. Wild-type nonneuronal cells extend survival of SOD1 mutant motor neurons in ALS mice. Science 2003;302:113–17
5. Lobsiger CS, Cleveland DW. Glial cells as intrinsic components of non-cell-autonomous neurodegenerative disease. Nat Neurosci 2003;10:1355–60
6. Ilieva H, Polymenidou M, Cleveland DW. Non–cell autonomous toxicity in neurodegenerative disorders: ALS and beyond. J Cell Biol 2009;187:761–72
7. Aguzzi A, Rajendran L. The transcellular spread of cytosolic amyloids, prions, and prionoids. Neuron 2009;64:783–90
8. Frost B, Diamond MI. Prion-like mechanisms in neurodegenerative diseases. Nat Rev Neurosci 2010;11:155–59
9. Urushitani M, Sik A, Sakurai T, et al. Chromogranin-mediated secretion of mutant superoxide dismutase proteins linked to amyotrophic lateral sclerosis. Nat Neurosci 2006;9:108–18
10. Urushitani M, Ezzi SA, Julien JP. Therapeutic effects of immunization with mutant superoxide dismutase in mice models of amyotrophic lateral sclerosis. Proc Natl Acad Sci U S A 2007;104:2495–500
11. Cao C, Lin X, Wahi MM, et al. Successful adjuvant-free vaccination of BALB/c mice with mutated amyloid beta peptides. BMC Neurosci 2008;9:25
12. Kutzler MA, Cao C, Bai Y, et al. Mapping of immune responses following wild-type and mutant Abeta42 plasmid or peptide vaccination in different mouse haplotypes and HLA class II Tg mice. Vaccine 2006;24:4630–39
13. He BP, Wen W, Strong MJ. Activated microglia (BV-2) facilitation of TNF-alpha–mediated motor neuron death in vitro. J Neuroimmunol 2002;128:31–38
14. Mir M, Asensio VJ, Tolosa L, et al. Tumor necrosis factor alpha and interferon gamma cooperatively induce oxidative stress and motoneuron death in rat spinal cord embryonic explants. Neuroscience 2009;162:959–71
15. Zhao W, Xie W, Xiao Q, et al. Protective effects of an anti-inflammatory cytokine, interleukin-4, on motoneuron toxicity induced by activated microglia. J Neurochem 2006;99:1176–87
16. Kawamata T, Akiyama H, Yamada T, et al. Immunologic reactions in amyotrophic lateral sclerosis brain and spinal cord tissue. Am J Pathol 1992;140:691–707
17. Beers DR, Henkel JS, Zhao W, et al. $CD4^+$ T cells support glial neuroprotection, slow disease progression, and modify glial morphology in an animal model of inherited ALS. Proc Natl Acad Sci U S A 2008;105:15558–63
18. Chiu IM, Chen A, Zheng Y, et al. T lymphocytes potentiate endogenous neuroprotective inflammation in a mouse model of ALS. Proc Natl Acad Sci U S A 2008;105:17913–18
19. Banerjee R, Mosley RL, Reynolds AD, et al. Adaptive immune neuroprotection in G93A-SOD1 amyotrophic lateral sclerosis mice. PLoS One 2008;3:e2740
20. Rakhit R, Robertson J, Vande Velde C, et al. An immunological epitope selective for pathological monomer-misfolded SOD1 in ALS. Nat Med 2007;13:754–59
21. Furukawa Y, O'Halloran TV. Amyotrophic lateral sclerosis mutations have the greatest destabilizing effect on the apo- and reduced form of SOD1, leading to unfolding and oxidative aggregation. J Biol Chem 2004;279:17266–74

22. Urushitani M, Kurisu J, Tateno M, et al. CHIP promotes proteasomal degradation of familial ALS-linked mutant SOD1 by ubiquitinating Hsp/Hsc70. J Neurochem 2004;90:231–44
23. Shibata N, Hirano A, Kobayashi M, et al. Presence of Cu/Zn superoxide dismutase (SOD) immunoreactivity in neuronal hyaline inclusions in spinal cords from mice carrying a transgene for Gly93Ala mutant human Cu/Zn SOD. Acta Neuropathol 1998;95:136–42
24. Gruzman A, Wood WL, Alpert E, et al. Common molecular signature in SOD1 for both sporadic and familial amyotrophic lateral sclerosis. Proc Natl Acad Sci U S A 2007;104:12524–29
25. Fujiwara N, Nakano M, Kato S, et al. Oxidative modification to cysteine sulfonic acid of Cys111 in human copper-zinc superoxide dismutase. J Biol Chem 2007;282:35933–44
26. Sato T, Takeuchi S, Saito A, et al. Axonal ligation induces transient redistribution of TDP-43 in brainstem motor neurons. Neuroscience 2009;164:1565–78
27. Tiwari A, Liba A, Sohn SH, et al. Metal deficiency increases aberrant hydrophobicity of mutant superoxide dismutases that cause amyotrophic lateral sclerosis. J Biol Chem 2009;284:27746–58
28. Baldridge JR, Yorgensen Y, Ward JR, et al. Monophosphoryl lipid A enhances mucosal and systemic immunity to vaccine antigens following intranasal administration. Vaccine 2000;18:2416–25
29. Ferri A, Nencini M, Cozzolino M, et al. Inflammatory cytokines increase mitochondrial damage in motoneuronal cells expressing mutant SOD1. Neurobiol Dis 2008;32:454–60
30. Ford L, Rowe D. Interleukin-12 and interferon-gamma are not detectable in the cerebrospinal fluid of patients with amyotrophic lateral sclerosis. Amyotroph Lateral Scler Other Motor Neuron Disord 2004;5:118–20
31. Rivest S. Regulation of innate immune responses in the brain. Nat Rev Immunol 2009;9:429–39
32. Racz I, Nadal X, Alferink J, et al. Interferon-gamma is a critical modulator of CB(2) cannabinoid receptor signaling during neuropathic pain. J Neurosci 2008;28:12136–45
33. Lobsiger CS, Boillee S, Cleveland DW. Toxicity from different SOD1 mutants dysregulates the complement system and the neuronal regenerative response in ALS motor neurons. Proc Natl Acad Sci U S A 2007; 104:7319–26
34. Ezzi SA, Urushitani M, Julien JP. Wild-type superoxide dismutase acquires binding and toxic properties of ALS-linked mutant forms through oxidation. J Neurochem 2007;102:170–78
35. Zhong Z, Deane R, Ali Z, et al. ALS-causing SOD1 mutants generate vascular changes prior to motor neuron degeneration. Nat Neurosci 2008; 11:420–22
36. Zeis T, Graumann U, Reynolds R, et al. Normal-appearing white matter in multiple sclerosis is in a subtle balance between inflammation and neuroprotection. Brain 2008;131:288–303
37. Kipnis J, Avidan H, Caspi RR, et al. Dual effect of $CD4^+CD25^+$ regulatory T cells in neurodegeneration: A dialogue with microglia. Proc Natl Acad Sci U S A 2004;101:14663–69
38. Gao X, Gillig TA, Ye P, et al. Interferon-gamma protects against cuprizone-induced demyelination. Mol Cell Neurosci 2000;16:338–49
39. Nicholas RS, Stevens S, Wing MG, et al. Microglia-derived IGF-2 prevents TNFα induced death of mature oligodendrocytes in vitro. J Neuroimmunol 2002;124:36–44
40. Baron R, Nemirovsky A, Harpaz I, et al. IFN-gamma enhances neurogenesis in wild-type mice and in a mouse model of Alzheimer's disease. FASEB J 2008;22:2843–52
41. Babu GN, Kumar A, Chandra R, et al. Elevated inflammatory markers in a group of amyotrophic lateral sclerosis patients from northern India. Neurochem Res 2008;33:1145–49
42. Hozumi H, Asanuma M, Miyazaki I, et al. Protective effects of interferon-gamma against methamphetamine-induced neurotoxicity. Toxicol Lett 2008;177:123–29
43. Takeuchi H, Wang J, Kawanokuchi J, et al. Interferon-gamma induces microglial-activation–induced cell death: A hypothetical mechanism of relapse and remission in multiple sclerosis. Neurobiol Dis 2006;22:33–39
44. Shechter R, London A, Varol C, et al. Infiltrating blood-derived macrophages are vital cells playing an anti-inflammatory role in recovery from spinal cord injury in mice. PLoS Med 2009;6:e1000113
45. Weiner HL, Lemere CA, Maron R, et al. Nasal administration of amyloid-beta peptide decreases cerebral amyloid burden in a mouse model of Alzheimer's disease. Ann Neurol 2000;48:567–79
46. Haenggeli C, Julien JP, Mosley RL, et al. Therapeutic immunization with a glatiramer acetate derivative does not alter survival in G93A and G37R SOD1 mouse models of familial ALS. Neurobiol Dis 2007;26:146–52
47. Habisch HJ, Schwalenstöcker B, Danzeisen R, et al. Limited effects of glatiramer acetate in the high-copy number hSOD1-G93A mouse model of ALS. Exp Neurol 2007;206:288–95
48. Meininger V, Drory VE, Leigh PN, et al. Glatiramer acetate has no impact on disease progression in ALS at 40 mg/day: A double- blind, randomized, multicentre, placebo-controlled trial. Amyotroph Lateral Scler 2009;10:378–83
49. Angelov DN, Waibel S, Guntinas-Lichius O, et al. Therapeutic vaccine for acute and chronic motor neuron diseases: implications for amyotrophic lateral sclerosis. Proc Natl Acad Sci U S A 2003;100:4790–95
50. Appel SH, Beers DR, Henkel JS. T cell-microglial dialogue in Parkinson's disease and amyotrophic lateral sclerosis: Are we listening? Trends Immunol 2010;31:7–17
51. Bhowmick S, Mazumdar T, Ali N. Vaccination route that induces transforming growth factor beta production fails to elicit protective immunity against *Leishmania donovani* infection. Infect Immun 2009;77: 1514–23

Phosphorylated TDP-43 in Frontotemporal Lobar Degeneration and Amyotrophic Lateral Sclerosis

Masato Hasegawa, PhD,[1] Tetsuaki Arai, MD, PhD,[2] Takashi Nonaka, PhD,[1] Fuyuki Kametani, PhD,[1] Mari Yoshida, MD, PhD,[3] Yoshio Hashizume, MD, PhD,[3] Thomas G. Beach, MD, PhD,[4] Emanuele Buratti, PhD,[5] Francisco Baralle, MD, PhD,[5] Mitsuya Morita, MD, PhD,[6] Imaharu Nakano, MD, PhD,[6] Tatsuro Oda, MD, PhD,[7] Kuniaki Tsuchiya, MD, PhD,[8] and Haruhiko Akiyama, MD, PhD[2]

Objective: TAR DNA-binding protein of 43kDa (TDP-43) is deposited as cytoplasmic and intranuclear inclusions in brains of patients with frontotemporal lobar degeneration with ubiquitinated inclusions (FTLD-U) and amyotrophic lateral sclerosis (ALS). Previous studies reported that abnormal phosphorylation takes place in deposited TDP-43. The aim of this study was to identify the phosphorylation sites and responsible kinases, and to clarify the pathological significance of phosphorylation of TDP-43.

Methods: We generated multiple antibodies specific to phosphorylated TDP-43 by immunizing phosphopeptides of TDP-43, and analyzed FTLD-U and ALS brains by immunohistochemistry, immunoelectron microscopy, and immunoblots. In addition, we performed investigations aimed at identifying the responsible kinases, and we assessed the effects of phosphorylation on TDP-43 oligomerization and fibrillization.

Results: We identified multiple phosphorylation sites in carboxyl-terminal regions of deposited TDP-43. Phosphorylation-specific antibodies stained more inclusions than antibodies to ubiquitin and, unlike existing commercially available anti–TDP-43 antibodies, did not stain normal nuclei. Ultrastructurally, these antibodies labeled abnormal fibers of 15nm diameter and on immunoblots recognized hyperphosphorylated TDP-43 at 45kDa, with additional 18 to 26kDa fragments in sarkosyl-insoluble fractions from FTLD-U and ALS brains. The phosphorylated epitopes were generated by casein kinase-1 and -2, and phosphorylation led to increased oligomerization and fibrillization of TDP-43.

Interpretation: These results suggest that phosphorylated TDP-43 is a major component of the inclusions, and that abnormal phosphorylation of TDP-43 is a critical step in the pathogenesis of FTLD-U and ALS. Phosphorylation-specific antibodies will be powerful tools for the investigation of these disorders.

Ann Neurol 2008;64:60–70

Tau-negative and ubiquitin-positive inclusions (UPIs) that include neuronal cytoplasmic inclusions (NCIs), neuronal intranuclear inclusions (NIIs), and dystrophic neurites (DNs) are the pathological hallmarks of frontotemporal lobar degeneration with ubiquitinated inclusions (FTLD-U) with or without clinical features of motor neuron disease (MND).[1] Recently, several genes and chromosomal loci, including the progranulin *(PGRN)* gene,[2,3] valosin-containing protein *(VCP)* gene,[4] and an unidentified site at chromosome 9p,[5,6] have been reported to be associated with familial FTLD-U. Ubiquitin-positive, tau-negative NCIs have also been recognized in patients with the classic type of MND, amyotrophic lateral sclerosis (ALS),[7] in which skein-like cytoplasmic inclusions are found in the lower motor neurons of the hypoglossal nucleus and spinal cord.[8,9] In both FTLD-U and ALS, understanding why these inclusions form may provide critical clues to the neurodegenerative process.

Recently, TAR DNA-binding protein of 43kDa

From the Departments of [1]Molecular Neurobiology and [2]Psychogeriatrics, Tokyo Institute of Psychiatry, Tokyo Metropolitan Organization for Medical Research, Kamikitazawa, Setagaya-ku, Tokyo; [3]Department of Neuropathology, Institute for Medical Science of Aging, Aichi Medical University, Yazako, Nagakute-cho, Aichi-gun, Aichi, Japan; [4]Sun Health Research Institute, Sun City, AZ; [5]International Centre for Genetic Engineering and Biotechnology, Trieste, Italy; [6]Department of Neurology, Jichi Medical University, Shimotsuke-shi, Tochigi; [7]Department of Neuropsychiatry, National Shimofusa Mental Hospital, Chiba; and [8]Department of Laboratory Medicine and Pathology, Tokyo Metropolitan Matsuzawa Hospital, Setagaya-ku, Tokyo, Japan.

Received Nov 8, 2007, and in revised form April 8, 2008. Accepted for publication April 22, 2008.

Published online in Wiley InterScience (www.interscience.wiley.com). DOI: 10.1002/ana.21425

Address correspondence to Drs Hasegawa and Arai, Departments of Molecular Neurobiology and Psychogeriatrics, Tokyo Institute of Psychiatry, Tokyo Metropolitan Organization for Medical Research, 2-1-8 Kamikitazawa, Setagaya-ku, Tokyo 156-8585. E-mail: masato@prit.go.jp

(TDP-43), which functions in regulating transcription and alternative splicing,[10,11] was identified as a component of these UPIs.[12–14] TDP-43 appears to belong to the group of two RNA-binding domain-Gly RNA-binding proteins, which include the heterogeneous nuclear ribonucleoprotein (hnRNP) family and factors involved in RNA splicing and transport.[15] TDP-43 binds hnRNP A/B and hnRNP A1 through its C-terminal region, inhibiting premessenger RNA splicing.[16] Several disorders, including FTLD-U, FTLD-MND, and ALS are now referred to as TDP-43 proteinopathies.[12–14] Immunoblot analysis of the sarkosyl-insoluble fraction extracted from brains of patients afflicted with these disorders shows an abnormal TDP-43–immunoreactive band at 45kDa. The electric mobility of this band changes after dephosphorylation, suggesting that abnormal phosphorylation takes place in accumulated TDP-43.[12,13] However, the phosphorylation sites, responsible kinases, and pathological significance of phosphorylation are still unknown.

In this report, we demonstrate that multiple antibodies raised against TDP-43 phosphopeptides label UPIs in histological sections from FTLD-U and ALS brains. These antibodies may offer advantages over previous antibodies used to identify these structures because they appear to be more sensitive than anti-ubiquitin antibodies and, unlike commercially available anti–TDP-43 antibodies, do not stain normal neuronal nuclei. In addition, these antibodies specifically recognize abnormal TDP-43 species on immunoblots of sarkosyl-insoluble fractions extracted from FTLD-U and ALS brains. Furthermore, we show that the multiple phosphorylation epitopes identified in aggregated TDP-43 are generated by casein kinase-1 (CK1), and that oligomerization or fibril formation of TDP-43 is promoted by phosphorylation with CK1 in vitro. These results suggest that phosphorylated TDP-43 is a critical component of UPIs in FTLD-U and ALS, and that phosphorylation of TDP-43 by CK1 may be involved in the accumulation of the protein.

Subjects and Methods

Materials

Human brain tissue was obtained from the Brain Donation Program at Sun Health Research Institute (Sun City, AZ), Aichi Medical University (Japan), Jichi Medical University (Japan), National Shimofusa Mental Hospital (Japan), and Tokyo Metropolitan Matsuzawa Hospital (Japan). Small blocks of brain tissue were dissected at autopsy and frozen rapidly at −70 to 80°C or fixed in 4% paraformaldehyde in 0.1M phosphate buffer (pH 7.4) for 2 days. Brain tissue from sporadic FTLD-U, familial FTLD-U with PGRN mutations (mPGRN), sporadic ALS, and sporadic FTLD-MND was compared with brain tissue from Alzheimer's disease (AD) and neurologically normal control subjects. The age, sex, brain regions examined, diagnosis, and histopathological subtyping for these cases are given in Table 1. Neuropathological diagnoses of FTLD-U, FTLD-MND, ALS, and AD were made in accordance with published guidelines.[1,9,17–19]

Table 1. **Subjects, Brain Regions, Pathological Diagnosis, and Subtypes Examined**

Case No.	Age (yr)	Sex	Region	Diagnosis	Subtype
1	67	M	Hip, T, F	FTLD-U (sporadic)	1
2	59	M	Hip, T	FTLD-U (sporadic)	1
3	68	F	Hip, T	FTLD-U (sporadic)	1
4	49	F	T	FTLD-MND	2
5	76	M	Prec	FTLD-MND	2
6	66	M	F, SC	ALS	2
7	70	M	Prec, SC	ALS	2
8	69	M	Prec	ALS	2
9	53	M	Hip, T, F	FTLD-U (mRGRN)	3
10	56	F	Hip, T, F	FTLD-U (mRGRN)	3
11	54	M	Hip, T, F	FTLD-U (mRGRN)	3
12	68	F	Hip, T	AD	—
13	83	F	Hip, T	AD	—
14	65	M	Hip, T	Control	—
15	72	M	Hip, T	Control	—

Hip = hippocampus; T = temporal; F = frontal; FTLD-U = frontotemporal lobar degeneration with ubiquitinated inclusions; MND = motor neuron disease; Prec = precentral; SC = spinal cord; ALS = amyotrophic lateral sclerosis; mPGRN = mutations of progranulin gene; AD = Alzheimer's disease.

Although none of the three ALS cases had a documented history of dementia, all had immunohistochemical evidence of pathology in the neocortex.

Preparation of Antibodies

Immunogens consisted of 39 synthetic phosphopeptides representing 36 of the 64 Ser/Thr/Tyr sites in the human TDP-43 molecule. All peptides were conjugated at the amino or carboxyl terminal by a cysteine linkage to synthetic thyroglobulin using m-maleimidobenzoyl-*N*-hydroxysuccinimide ester as a coupling reagent.[20] The rabbit antisera were purified by obtaining flow-through fractions from a Toyopearl AF-Tresyl-650M (TOSOH, Tokyo, Japan) or SulfoLink Coupling Gel (Pierce Biotechnology, Rockford, IL) precoated with the nonphosphorylated synthetic peptide. The specificities of the antibodies were verified by enzyme-linked immunosorbent assay and immunoblot. A phosphorylation-independent rabbit polyclonal antibody to TDP-43 was also produced using a C-terminal peptide of TDP-43 (405-414) as immunogen.

Immunohistochemistry

After cryoprotection in 15% sucrose in 0.01M phosphate-buffered saline (pH 7.4), paraformaldehyde-fixed tissue blocks were cut on a freezing microtome at 30μm thickness. The free-floating sections were immunostained with an anti-ubiquitin antibody (DF2, a gift from Dr Mori, 1:200),[21] a commercially obtained phosphorylation-independent anti–TDP-43 antibody (10782-1-AP; ProteinTech Group, Chicago, IL; 1:2,000), and a panel of phosphorylation-dependent anti–TDP-43 antibodies including pS409/410, using methods previously described.[13] Double-labeled immunofluorescence was performed using fluorescein isothiocianate– and tetramethylrhodamine isothiocyanate–conjugated secondary antibodies; sections were examined with a confocal laser microscope (LSM5 PASCAL; Carl Zeiss MicroImaging GmbH, Jena, Germany).

Immunoelectron Microscopy

Tissue blocks of ALS lumber spinal cord were fixed in paraformaldehyde and embedded in LR White Resin (London Resin, Reading, United Kingdom). Ultrathin sections were incubated with pS409/410 (1:1,000), and the immunoreaction products were probed using colloidal gold particles (1:10 dilution; BBinternational, Cardiff, United Kingdom) according to a standard immunogold-based postembedding electron microscopic procedure.[22]

Immunoblotting

Sarkosyl-insoluble, urea-soluble fractions were extracted from the frontal and the temporal regions of control, FTLD-U, and ALS brains as previously described.[23] The samples before (−) and after (+) the treatment with lambda protein phosphatase (λPPase) were loaded on 10% sodium dodecyl sulfate polyacrylamide gel electrophoresis. Proteins in the gel were then electrotransferred onto a polyvinylidene difluoride membrane (Millipore, Bedford, MA). After blocking with 3% gelatin in tris(hydroxymethyl)aminomethane (Tris)–buffered saline (50mM Tris-HCl, pH 7.5, 150mM NaCl), membranes were incubated overnight with the primary antibodies. After incubation with an appropriate biotinylated secondary antibody, labeling was detected as described previously.[13,23]

In Vitro Phosphorylation and Fibrillization of TDP-43

Human TDP-43 complementary DNA were subcloned into pRK172 expression vectors and transformed into *Escherichia coli* BL21(DE3). For in vitro phosphorylation, crude extracts from *E. coli* that expressed human TDP-43 were used to prepare partially purified TDP-43 using heparin-Toyopearl column chromatography and elution with 0.5M NaCl. The elutes were phosphorylated with CK1 (10,000U/ml; New England Biolabs, Beverly, MA), casein kinase-2 (CK2) (10,000U/ml; New England Biolabs), or glycogen synthase kinase-3β (GSK3β) (10,000U/ml; New England Biolabs) at 30°C for 14 hours. To study fibrillization, we incubated partially purified TDP-43 aliquots in 30mM Tris-HCl at pH 7.5 containing 4mM magnesium chloride, 2mM ATP, with or without CK1 (10,000U/ml) at 30°C for 3 days. A few drops of reaction solution was then applied to a carbon-coated copper grid and allowed to air-dry. The grid was placed on a drop of blocking solution (10mg/ml bovine serum albumin in phosphate-buffered saline) for 10 minutes and then placed on a drop of primary antibody (pS409/410, 1:200) for 2 hours at room temperature. After washing with 10mg/ml bovine serum albumin in phosphate-buffered saline, the grid was placed on a drop of the secondary antibody conjugated to 10nm colloidal gold particles (1:50; Sigma, St. Louis, MO) for 1 hour at room temperature. Finally, after another round of washing, the grid was negatively stained with 2% sodium phosphotungstate and examined with the electron microscopy (JEM-1230; JEOL, Akishime, Japan).

Results

Multiple Sites within TDP-43 Are Abnormally Phosphorylated in Frontotemporal Lobar Degeneration with Ubiquitinated Inclusions and Amyotrophic Lateral Sclerosis

There are multiple potential phosphorylation sites within human TDP-43, including 41 serine (Ser), 15 threonine (Thr), and 8 tyrosine (Tyr) residues. To identify the critical phosphorylation sites of TDP-43, we raised antibodies against 39 different synthetic phosphopeptides, representing 36 of 64 candidate phosphorylation sites (Table 2). The major strategy was to choose Ser and Thr residues that cover known protein kinase consensus phosphorylation motifs, including R-X-pSer/Thr for protein kinase A, pSer/Thr-X-X-Ser/Thr for CK1, pSer/Thr-X-X-E/D for CK2, and pSer/Thr-X-X-X-Ser for GSK3 and CK1. In addition, Ser/Thr residues in C-terminal region of TDP-43 were chosen because they are analogous to abnormal phosphorylation sites found in tau or α-synuclein.

Of the generated antibodies, pS379, pS403/404, pS409, pS410, and pS409/410 intensely immunostained the UPIs in FTLD-U and ALS, and demonstrated, on immunoblots of sarkosyl-insoluble fractions

Table 2. **Antigen Peptides for Immunization of Rabbits**

	Site	Antigen Peptide
1	pT8	EYIRVT(p)EDENDEC
2	pS20	PIEIPS(p)EDDGTC
3	pS29	GTVLLS(p)TVTAC
4	pT88	CNYPKDNKRKMDET(p)D
5	pS91	CDETDAS(p)SAVKVKR
6	pS92	CDETDASS(p)AVKVKR
7	pS91/92	DETDAS(p)S(p)AVKVC
8	pT103	CKRAVQKT(p)SDLIVLG
9	pS104	CKRAVQKTS(p)DLIVLG
10	pT116	PWKTT(p)EQDLKEC
11	pT141	KKDLKT(p)GHSKGC
12	pT153	CGFVRFT(p)EYETQVK
13	pS180	CKLPNS(p)KQSQDE
14	pS183	CPNSKQS(p)QDEPLR
15	pS190	CKQSQDEPLRS(p)RK
16	pT199	CT(p)EDMTEDLE
17	pT203	RCTEDMT(p)EDELR
18	pT233	CRAFADVT(p)FADDQ
19	pS254	IIKGIS(p)VKISC
20	pS258	CISVHIS(p)NAEPK
21	pS266	CPKHNS(p)NRQLER
22	pS273	CRQLERS(p)GRFGGN
23	pS292	CGFGNS(p)RGGGA
24	pS305	CNNQGS(p)NMGGG
25	pS317	CFGAFS(p)INPAM
26	pS332	CAALQS(p)SWGMM
27	pS350	CQSGPS(p)GNNQN
28	pS375	GNNSYS(p)GSNSGC
29	pS379	CSGSNS(p)GAAIG
30	pS389	CGWGSAS(p)NAGS
31	pS393	CASNAGS(p)GSGF
32	pS395	CAGSGS(p)GFNGG
33	pS403	CGFNGGFGS(p)SMD
34	pS404	CNGGFGSS(p)MDSK
35	pS403/404	CNGGFGS(p)S(p)MDSK
36	pS407	CGSSMDS(p)KSSGW
37	pS409	CMDSKS(p)SGWGM
38	pS410	CMDSKSS(p)GWGM
39	pS409/410	CMDSKS(p)S(p)GWGM

extracted from brains of the FTLD-U and ALS cases, an abnormal band of 45kDa but not the 43kDa band corresponding to normal TDP-43. The results suggest that these sites are phosphorylated in the abnormal aggregates of TDP-43 present in FTLD-U and ALS.

Immunohistochemical Characterization of Phosphorylated TDP-43

Immunohistochemical staining showed that five of the phosphorylation-specific anti-TDP-43 antibodies identified UPIs in both FTLD-U and ALS brains. Of the phosphorylation-specific antibodies, the immunoreactivity of pS409/410 was particularly robust (Fig 1). In comparison, the commercially obtained, phosphorylation-independent, anti–TDP-43 antibody labeled NCIs, DNs, and neuronal nuclei in the dentate gyrus (see Fig 1A) and the temporal cortex (see Fig 1B) of the sporadic FTLD-U cases, and skein-like inclusions and neuronal nuclei in the spinal cord of ALS cases (see Fig 1C). It was particularly difficult to distinguish the staining of NCIs from that of neuronal nuclei in the dentate gyrus of the sporadic FTLD-U cases (see Fig 1A). By contrast, NCIs and DNs were unambiguously identified by the phosphorylation-specific antibody pS409/410, with no nuclear staining (see Figs 1D, E). Similarly, pS409/410 clearly labeled skein-like (see Fig 1F) and glial inclusions (see Fig 1G) in the spinal cord, and NCIs in the frontal and precentral cortices of the FTLD-MND and ALS cases (see Fig 1H). Glial inclusions in the frontal and precentral regions of the FTLD-MND and ALS cases were also immunopositive (data not shown). In the cases of familial FTLD-U with PGRN mutations, pS409/410 intensely stained NCIs, DNs, and NIIs in the cerebral cortex (see Figs 1I–K) and abundant positive structures in the cerebral white matter (see Fig 1L). The results of double-immunofluorescence staining showed that pS409/410 identified more NCIs than the ubiquitin antibody (see Figs 1M–O).

Based on morphological aspects, TDP-43 proteinopathies have been classified into four subtypes.[24] Type 1 is characterized by DNs with few NCIs and no NIIs, type 2 has numerous NCIs with few DNs and no NIIs, type 3 has numerous NCIs and DNs and an occasional NII, and type 4 has numerous NIIs and DNs with few NCIs. Type 4 is specific for familial FTLD-U with mutations of valosin-containing protein *(VCP)* gene. In this study, using the commercial anti–TDP-43 antibody, all of the sporadic FTLD-U cases showed type 1 pathology, all FTLD-MND and ALS cases showed type 2 pathology, and all FTLD-U with mPGRN showed type 3 pathology, in agreement with previous reports.[24,25]

The staining patterns obtained with our phosphorylation-dependent antibodies were similar to those seen

with the commercial phosphorylation-independent antibody, suggesting that all of the inclusion types previously described contain phosphorylated TDP-43. Similar staining patterns were obtained using pS379 (Figs 2A–C), pS403/404 (see Figs 2D–F), pS409 (see Figs 2G–I), and pS410 (see Figs 2J–L). Preabsorption of the antibodies with phosphopeptide immunogens abolished the labeling of these structures (data not shown).

Immunoelectron microscopic examination of the

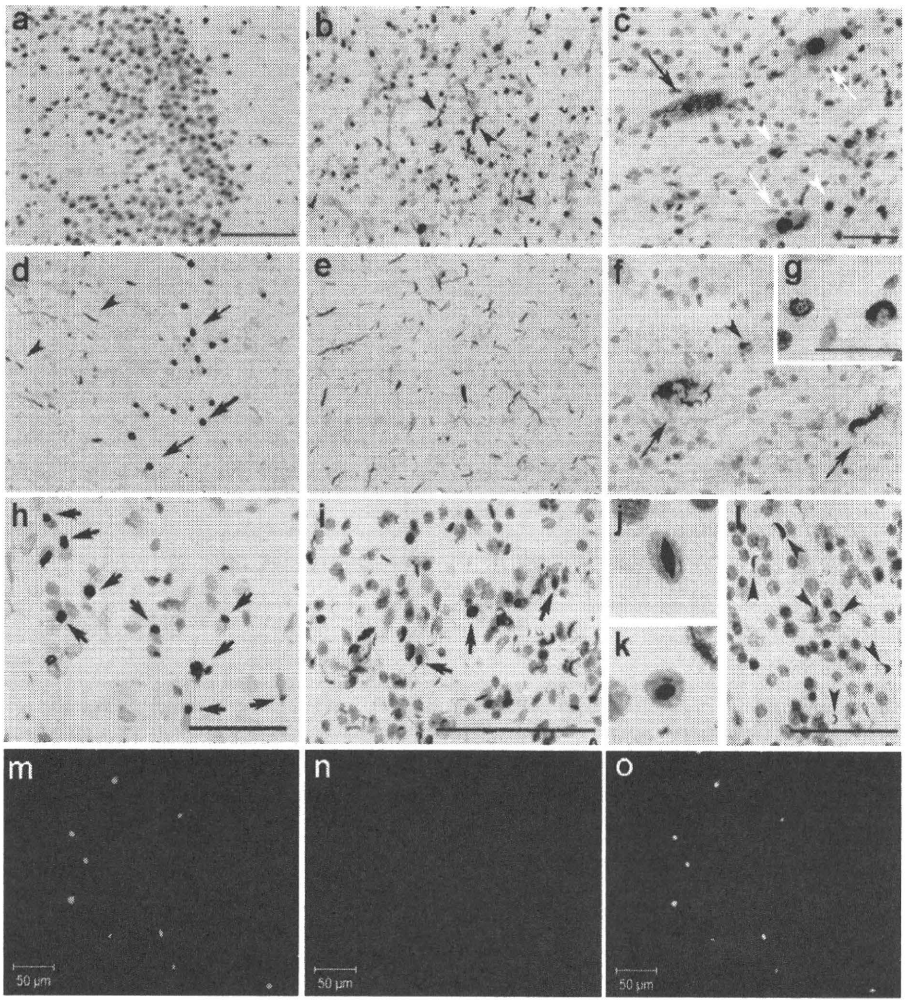

Fig 1. Immunohistochemical comparison of frontotemporal lobar degeneration with ubiquitinated inclusions (FTLD-U) and amyotrophic lateral sclerosis (ALS) brains using the phosphorylation-independent anti–TAR DNA-binding protein of 43kDa (TDP-43) antibody (ProteinTech) (A–C) and the phosphorylation-dependent anti–TDP-43 antibody (pS409/410) (D–L), in the dentate gyrus (A, D) and temporal cortex (B, E) of the sporadic FTLD-U cases, in the lumbar spinal cord (C, F, G) and the frontal cortex (H) of the ALS cases, and in the frontal cortex (I–K) and the frontal white matter (L) of the familial FTLD-U cases with progranulin (PGRN) mutations. (A) Because most of the nuclei of dentate gyrus granular neurons are immunopositive with the phosphorylation-independent antibody, it is difficult to identify neuronal cytoplasmic inclusions (NCIs). (B) TDP-43–positive dystrophic neurites (DNs) are recognizable (arrowheads) *in addition to the nuclei. (C) The* black arrow *indicates a cell with skein-like inclusions.* White arrows *and* arrowheads *indicate the normal nuclei of anterior horn cells and glial nuclei, respectively. Photomicrographs (D–F) illustrate the corresponding areas to (A–C), respectively. Note the absence of nuclear staining in (D–G) with the phosphorylation-dependent antibody pS409/410. (D) NCIs* (arrows) *and DNs* (arrowheads) *are clearly seen. (E) More abundant DNs are seen than in (B). (F)* Arrows *indicate skein-like inclusions;* arrowheads *indicate glial inclusions. (G, insert) Glial inclusions at a higher magnification. (H) NCIs in the frontal cortices of the ALS case are immunopositive. In the cases with PGRN mutations, pS409/410 clearly stains NCIs* (arrows), *DNs (I), and neuronal intranuclear inclusions (NIIs) (J, K) in the superficial cortical layers, and abundant immunopositive structures in the white matter (L,* arrowheads*), with no nuclear staining. Sections are counterstained with hematoxylin to show nuclei in (C, F–L). (M–O) Antiubiquitin (DF2) and pS409/410 double-label immunofluorescence histochemistry of the dentate gyrus in the FTLD-U case. Only some of the pS409/410-positive NCIs are also ubiquitin positive. (M) DF2; (N) pS409/410; (G) merge. Cell nuclei are stained with TO-PRO-3 (Invitrogen, Tokyo, Japan), producing a blue color. Scale bars = 100μm (A, B, D, E, I); 50μm (C, F, H, L); 25μm (G); 10μm (J, K).*

spinal cord motoneuron inclusions of an ALS patient with the pS409/410 antibody showed immunopositive abnormal fibers of 15nm in diameter (Figs 3A, B).

Immunoblot Analysis of Phosphorylated TDP-43

Immunoblot analyses of sarkosyl-insoluble fractions extracted from the brains of control, AD, FTLD-U, and ALS cases with the phosphorylation-independent TDP-43 antibody (ProteinTech) always showed a band of 43kDa and also showed an additional 45kDa band that was present only in FTLD-U and ALS cases, as described previously[12,13] (Fig 4A). The phosphorylation-dependent antibodies specific for pS409/410 (see Fig 4B), pS409 (see Fig 4C), pS410 (see Fig 4D), pS403/404 (see Fig 4E), and pS379 (see Fig 4F) did not recognize the normal 43kDa band, showing a single band at approximately 45kDa, several smaller fragments at approximately 25kDa, and indistinct smears in FTLD-U and ALS cases but not in control and AD cases (see Figs 4B–F). The intensity of the approximately 25kDa fragments tended to be greater than that of the 45kDa band in FTLD-U (see Figs 4B–E) and in ALS (see Figs 4B, D). As for the immunohistochemical findings, the antibody to pS409/410 showed the most intense labeling (see Fig 4B). All of the immunoreactive bands were completely abolished by dephosphorylation, which was performed with lambda protein phosphatase (8,000U/ml; New England Biolabs) at 30°C for 2 hours.

Immunoblot Distinction between Clinicopathological Subtypes of TDP-43

To investigate the biochemical basis of the different TDP-43 clinicopathological subtypes, we have carefully compared the results of immunoblots of the sarkosyl-insoluble, urea-soluble fractions from cerebral cortex of sporadic FTLD-U, FTLD-MND, ALS, and mPGRN cases. The results showed that the band patterns of the 18 to 26kDa fragments differed between clinicopathological subtypes (Figs 5A, B). Sporadic FTLD-U cases showed 2 major bands at 23 and 24kDa, and 2 minor bands at 18 and 19kDa, whereas FTLD-MND and ALS cases showed 3 major bands at 23, 24, and 26kDa, and 2 minor bands at 18 and 19kDa. A 23kDa band is the most intense in sporadic FTLD-U, whereas a 24kDa band is the most intense in FTLD-MND and ALS. Furthermore, the band pattern of mPGRN cases was not distinctive but intermediate between FTLD-U, FTLD-MND, and ALS cases.

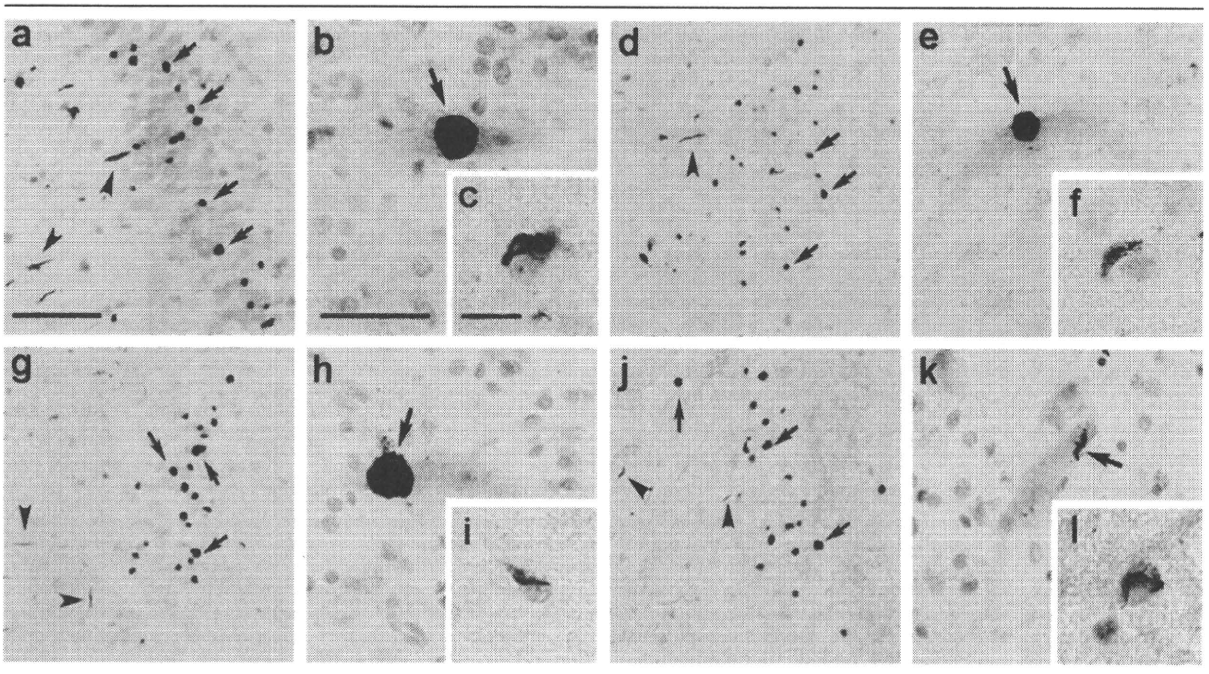

Fig 2. Immunohistochemistry of frontotemporal lobar degeneration with ubiquitinated inclusions (FTLD-U) brains and amyotrophic lateral sclerosis (ALS) spinal cords using the phosphorylation-dependent anti–TAR DNA-binding protein of 43kDa (TDP-43) antibodies specific for pS379 (A–C), pS403/404 (D–F), pS409 (G–I), and pS410 (J–L). These antibodies recognize neuronal cytoplasmic inclusions (NCIs) (arrows *in A, D, G, J) and dystrophic neurites (DNs)* (arrowheads *in A, D, G, J) in the dentate gyrus of the sporadic FTLD-U cases and motoneuronal round inclusions* (arrow *in B, E, H), skein-like inclusion (K,* arrow*), and glial inclusions (C, F, I, L) in the lumber spinal cord of the ALS cases. Note the absence of nuclear staining. Sections are counterstained with hematoxylin to show nuclei in (A–C, E, F, H, I, K, L). Scale bars = 100μm (A, D, G, J); 25μm (B, E, H, K); 12.5μm (C, F, I, L).*

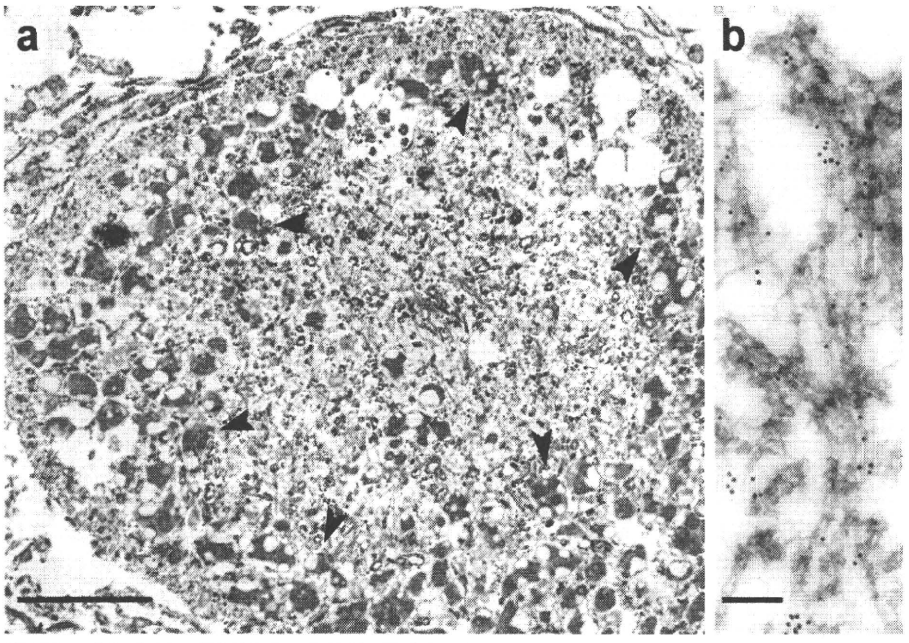

Fig 3. (A) A low-power immunoelectron micrograph of a phosphorylated TAR DNA-binding protein of 43kDa (TDP-43)–positive motoneuronal inclusion in the spinal cord of an amyotrophic lateral sclerosis (ALS) patient. The irregularly shaped structure surrounded by lipofuscins (arrowheads) *is the inclusion. (B) At higher magnification, abnormal filaments of 15nm in diameter are immunopositive. Immunoreaction with pS409/410, probed with immunogold particles (diameter 10nm), appears as* black dots. *Bars = 5μm (A); 500nm (B).*

Phosphorylation Epitopes Are Generated by Casein Kinase-1

To investigate the kinase responsible for the abnormal phosphorylation of TDP-43, we treated recombinant TDP-43 in vitro with CK1, CK2, and GSK3β. Immunoblot analyses of the recombinant TDP-43 showed that phosphorylation by CK1 caused a reduction in gel mobility of TDP-43 to approximately 45kDa and strong immunoreactivity to the phosphorylation-specific antibodies (Fig 6A). TDP-43 phosphorylated by CK2 was only weakly immunoreactive for these antibodies (see Fig 6A), and that phosphorylated by GSK3β was negative (data not shown). Kinase activity capable of generating the approximately 45kDa TDP-43 with pS409/410 epitopes was also detected in crude rat brain extracted with a high concentration (10–20mM) of $MgCl_2$ (data not shown). This kinase activity was not inhibited by the CK2 inhibitor heparin, suggesting that CK1 may be the major kinase in brain extract. Interestingly, increased levels of sodium dodecyl sulfate–stable TDP-43 oligomers were observed after phosphorylation by CK1 (see Fig 6B). Furthermore, based on immunoelectron microscopic analysis, recombinant TDP-43 phosphorylated by CK1 formed abundant filaments when applied on a carbon-coated copper grid (see Fig 6C), whereas nonphosphorylated recombinant TDP-43 formed few filaments (data not shown).

Discussion

We show here that antibodies generated to multiple TDP-43 phosphorylation sites stain the pathological structures in FTLD-U and ALS. These structures include NCIs, NIIs, and DNs in the cerebral cortex and hippocampus, as well as skein-like, round, and glial inclusions in the spinal cord. The phosphorylation-dependent antibodies stain these structures more extensively than an anti-ubiquitin antibody and do not stain normal neuronal nuclei. Furthermore, on immunoelectron microscopy, the phosphorylation-dependent antibodies label abnormal filaments in the motoneuronal inclusion of the ALS case, although these findings may not be the same as for other types of cytoplasmic and intranuclear inclusions.[26] Immunoblot analysis of sarkosyl-insoluble fractions from FTLD-U and ALS brains shows that these antibodies specifically stain abnormal TDP-43 species. These findings are therefore analogous to previous discoveries of phosphorylation-specific epitopes for tau and α-synuclein in tauopathies and α-synucleinopathies.[27–29]

At least five sites on TDP-43 are phosphorylated (Ser 379, Ser 403/404, Ser 409/410) in subjects with FTLD-U and ALS. These results suggest that abnormal phosphorylation takes place mainly near the carboxyl (C)-terminal region of TDP-43. This again is similar to tauopathies and synucleinopathies,[27,28] where multiple Ser residues in the C-terminal region, including

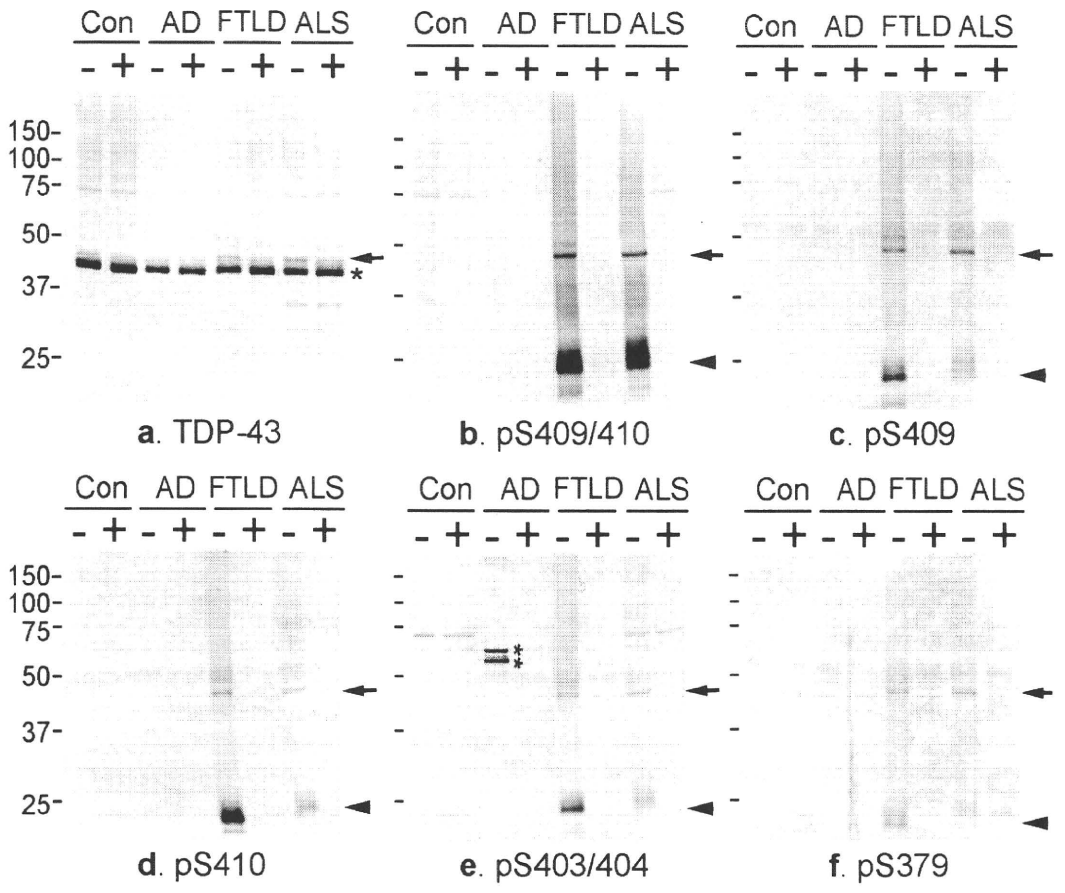

Fig 4. (A) Immunoblot analyses of sarkosyl-insoluble, urea-soluble fractions from control, Alzheimer's disease (AD), frontotemporal lobar degeneration (FTD; frontotemporal lobar degeneration with ubiquitinated inclusions [FTLD-U]), and amyotrophic lateral sclerosis (ALS) brains with phosphorylation-independent anti–TAR DNA-binding protein of 43kDa (TDP-43) antibody (Protein-Tech) (A) and phosphorylation-dependent anti–TDP-43 antibodies specific for pS409/410 (B), pS409 (C), pS410 (D), pS403/404 (E), and pS379 (F) before (−) and after (+) the treatment with lambda protein phosphatase (λPPase). (A) With the phosphorylation-independent antibody, a positive band of 43kDa is commonly seen (asterisk), *whereas an additional band of 45kDa is observed only in FTD and ALS* (arrow), *the labeling of which is abolished after dephosphorylation. (B–F) The phosphorylation-dependent antibodies specifically label the approximately 45kDa band* (arrow) *and the approximately 25kDa fragment* (arrowhead), *as well as a smear, only in FTD and ALS. These immunoreactivities are abolished after dephosphorylation. Normal 43kDa TDP-43 in control and diseased brains is not stained by these phosphorylation-dependent antibodies. The two bands recognized by the antibody specific for pS403/404 in AD (E,* double asterisk*) disappear after dephosphorylation, suggesting a cross-reaction of the antibody to other phosphorylated proteins.*

Ser422 in tau and C-terminal Ser129 in α-synuclein, are abnormally phosphorylated. It has been established that hyperphosphorylated tau and α-synuclein represent the earliest detectable molecular change in the brain in these neurodegenerative diseases.[29,30] Thus, the results of this study suggest that abnormally phosphorylated TDP-43 is a critical component of UPIs in FTLD-U and ALS.

There is a close relation between the pathological subtypes of TDP-43 proteinopathy and the immunoblot pattern of C-terminal fragments of phosphorylated TDP-43. These findings confirm and extend Sampathu and colleagues'[31] and Neumann and coworkers'[12] previous reports that showed C-terminal fragment composition varied between cases with type 1 and 2 pathology. Furthermore, we have shown that cases with type 3 pathology have a band pattern that is mixed or intermediate. These results parallel our earlier findings of differing C-terminal tau fragments in progressive supranuclear palsy and corticobasal degeneration, despite identical composition of tau isoforms.[32] Taken together, these results suggest that elucidating the mechanism of C-terminal fragment origination may shed light on the pathogenesis of several neurodegenerative disorders involving TDP-43 proteinopathy and tauopathy.

These phosphorylation-specific antibodies are a new and powerful tool for the investigation of TDP-43 pro-

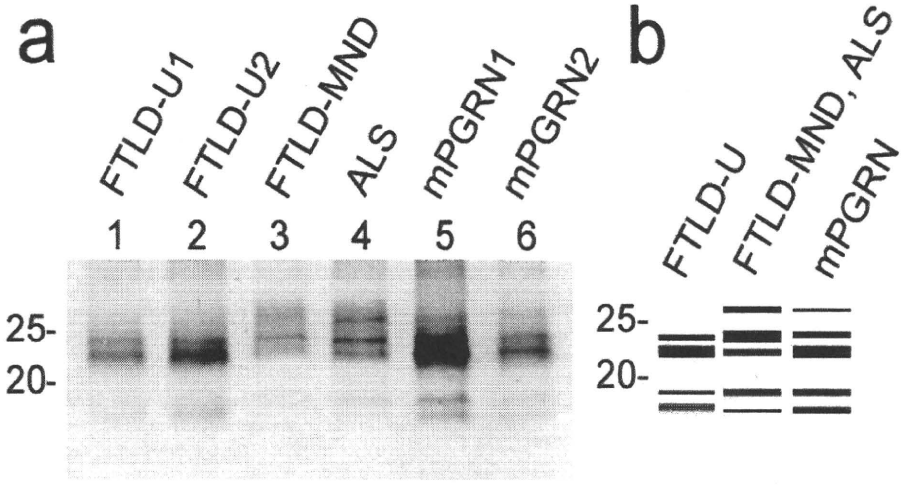

Fig 5. A relation between the clinicopathological subtypes of TAR DNA-binding protein of 43kDa (TDP-43) proteinopathies and the band pattern of the C-terminal fragments of phosphorylated TDP-43. (A) Immunoblots of the sarkosyl-insoluble, urea-soluble fractions from sporadic frontotemporal lobar degeneration with ubiquitinated inclusions (FTLD-U), FTLD-motor neuron disease (MND), amyotrophic lateral sclerosis (ALS), and progranulin mutations (mPGRN) cases with the pS409/410 antibody. The samples are loaded on 15% polyacrylamide gel. Sporadic FTLD-U cases (lanes 1, 2) show a band pattern with 2 major bands at 23 and 24kDa, and 2 minor bands at 18 and 19kDa. A band of 24kDa is weaker than that of 23kDa, and a 19kDa band is weaker than an 18kDa band. FTLD-MND (lane 3) and ALS (lane 4) cases show a pattern with 3 major bands at 23, 24, and 26kDa, and 2 minor bands at 18 and 19kDa. A 24kDa band is the most intense, and an 18kDa band is weaker than a 19kDa band. mPGRN (lanes 5, 6) cases show 3 major bands at 23, 24, and 26kDa, and 2 minor bands at 18 and 19kDa. A 23kDa band is the most intense, and a band of 18kDa and that of 19kDa show similar intensity. The band pattern of mPGRN cases is therefore a composite of that seen in FTLD-U, FTLD-MND, and ALS. (B) Schematic diagram of the band pattern of the C-terminal fragments of phosphorylated TDP-43.

teinopathies. Because phosphorylation-dependent antibodies to TDP-43 react only with abnormally deposited TDP-43, they offer advantages over existing commercially available antibodies for the pathological diagnosis and subtyping of TDP-43 proteinopathies. In addition, and again in analogy with tauopathies, these antibodies may be useful for detecting abnormal TDP-43 in biological fluids such as cerebrospinal fluid.[33]

The results suggest that CK1 is involved in the abnormal phosphorylation and accumulation of TDP-43. In this study, the treatment of recombinant TDP-43 by CK1 generates the same phosphorylation epitopes that are recognized by phosphorylation-dependent antibodies. In addition, phosphorylation at these epitopes facilitates filament formation. In comparison, several protein kinases have been reported to be responsible for phosphorylating tau and α-synuclein. They include, for tau phosphorylation,[34–37] GSK3β, cyclin-dependent kinase 5, mitogen-activated protein kinase, and mitogen-activated protein/microtubule affinity-regulating kinase, and for α-synuclein phosphorylation,[38–40] CK1, CK2, and G-protein–coupled receptor kinase 5.

The pathological significance of phosphorylation of TDP-43 is not clear. It is well known that protein phosphorylation plays an important role in regulating transcription and premessenger RNA splicing. Several splicing factors including hnRNPs, small nuclear ribonucleoproteins, and serine/arginine-rich protein family are known to be phosphorylated in vivo. Various kinases including CK1 have been implicated in phosphorylating these factors.[41–43] Phosphorylation of these factors modulates protein-protein and protein-RNA interactions, and affects their subcellular localization and physiological functions.[41] For instance, Habelhah and colleagues[44] showed that phosphorylation of hnRNP-K by extracellular-signal–regulated kinase results in its cytoplasmic accumulation and also inhibits messenger RNA translation. van der Houven van Oordt and coauthors reported that stress-induced activation of the mitogen-activated protein kinase kinase$_{3/6}$-p38 pathway causes hyperphosphorylation and cytoplasmic accumulation of hnRNP A1, affecting alternative splicing regulation.[45] Thus, phosphorylation of TDP-43 may lead to its cytoplasmic accumulation and influence various physiological functions. Currently, however, it is unclear whether TDP-43 is physiologically phosphorylated in brain. Although in HeLa cells, Ser91 and Ser92 of TDP-43 were reported to be phosphorylated,[46] the antibody specific to pS91/pS92 we made in this study did not stain any structures in normal brains (data not shown). Despite the normal nuclear location of TDP-43, none of the our five phosphorylation-

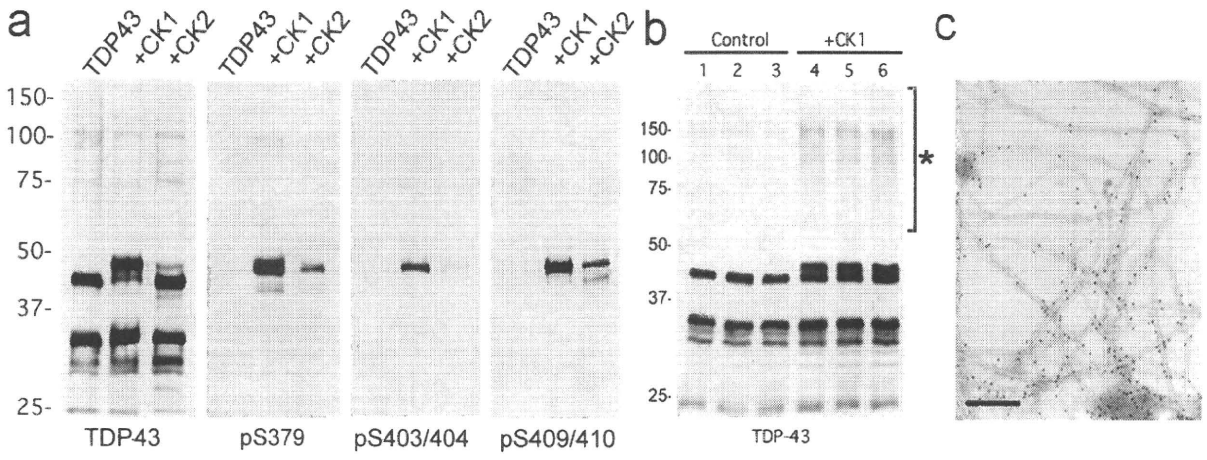

Fig 6. (A) Immunoblot analyses of recombinant TAR DNA-binding protein of 43kDa (TDP-43) phosphorylated in vitro. The crude extract from E. coli *that expressed human TDP-43 is treated with casein kinase-1 (CK1) and CK2 at 30°C for 14 hours, and probed with a phosphorylation-independent antibody against a C-terminal peptide of TDP-43 (405–414), and with phosphorylation-dependent antibodies pS379, pS403/404, and pS409/410. Phosphorylation by CK1 causes the mobility shift to approximately 45kDa and induction of intense immunoreactivity to the phosphorylation-dependent antibodies. (B) Immunoblot analyses of recombinant TDP-43 phosphorylated by CK1. The recombinant TDP-43, which is partially purified by heparin-Toyopearl column chromatography, is incubated with (lanes 4–6) or without (lanes 1–3) CK1 in the presence of adenosine triphosphate at 37°C for 14 hours, and probed with the phosphorylation-independent TDP-43 antibody (ProteinTech). Results in three independent, representative experiments are shown. Note the sodium dodecyl sulfate (SDS)–stable TDP-43 oligomers at approximately 100 to 200kDa* (asterisk) *are detected after phosphorylation by CK1. (C) Positive immunolabeling by pS409/410 of filaments assembled from recombinant TDP-43 phosphorylated by CK1 (10nm colloidal gold). Scale bar = 200nm.*

dependent antibodies stained normal nuclei, suggesting that phosphorylation of these sites is a disease-specific phenomenon.

Our in vitro studies suggest that phosphorylation of TDP-43 facilitates the formation of sodium dodecyl sulfate–stable oligomers and filaments of TDP-43. These abnormal structures may be neurotoxic, as suggested previously for tauopathies and α-synucleinopathies.[30] Thus, abnormal phosphorylation of TDP-43 may be pathological through either a loss of function or a toxic gain of function, or both, leading to the characteristic neuronal degeneration and clinical syndromes.

This research was supported by the Ministry of Education, Culture, Sports, Science and Technology of Japan (Grant-in-Aid for Scientific Research on Priority Areas–Research on Pathomechanisms of Brain Disorders, M.H. (20023038); a Grant-in-Aid for Scientific Research, M.H. (18300117); Grants-in-Aid for Scientific Research, T.A. (19591024), T.N. (19590299)); Grants-in-Aid from the Research Committee of CNS Degenerative Diseases, the Ministry of Health, Labour and Welfare of Japan, I.N. and M.Y. (20261501); the Brain Donation Program at Sun Health Research Institute is supported by the NIH (National Institute on Aging, P30 AG19610), Arizona Alzheimer's Disease Core Center, the Arizona Department of Health Services (contract 211002, Arizona Alzheimer's Research Center), the Arizona Biomedical Research Commission (contracts 4001, 0011, and 05-901), and the Prescott Family Initiative of the Michael J. Fox Foundation for Parkinson's Research; F.B. and E.B. were supported by Telethon Onlus Foundation, Italy (GGP06147) and by a European Community Grant (EURASNET-LSHG-CT-2005-518238).

We thank H. Kondo and Y. Izumiyama for their excellent technical assistance.

References

1. Mackenzie IRA, Feldman HH. Ubiquitin immunohistochemistry suggests classic motor neuron disease, motor neuron disease with dementia, and frontotemporal dementia of the motor neuron disease type represent a clinicopathological spectrum. J Neuropathol Exp Neurol 2005;64:730–739.
2. Baker M, Mackenzie IR, Pickering-Brown SM, et al. Mutations in progranulin cause tau-negative frontotemporal dementia linked to chromosome 17. Nature 2006;442:916–919.
3. Cruts M, Gijselinck I, van der Zee J, et al. Null mutations in progranulin cause ubiquitin-positive frontotemporal dementia linked to chromosome 17q21. Nature 2006;442: 920–924.
4. Watts GDJ, Wymer J, Kovach MJ, et al. Inclusion body myopathy associated with Paget disease of bone and frontotemporal dementia is caused by mutant valosin-containing protein. Nat Genet 2004;36:377–381.
5. Morita M, Al-Chalabi A, Anderson PM, et al. A locus on chromosome 9p confers susceptibility to ALS and frontotemporal dementia. Neurology 2006;66:839–844.
6. Vance C, Al-Chalabi A, Ruddy D, et al. Familial amyotrophic lateral sclerosis with frontotemporal dementia is linked to a locus on chromosome 9p13.2-21.3. Brain 2006;129:868–875.
7. Leigh PN, Anderton BH, Dodson A, et al. Ubiquitin deposits in anterior horn cells in motor neurone disease. Neurosci Lett 1988;93:197–203.
8. Lowe J, Lennox G, Jefferson D, et al. A filamentous inclusion body within anterior horn neurones in motor neurone disease defined by immunocytochemical localization of ubiquitin. Neurosci Lett 1988;94:203–210.

9. Piao YS, Wakabayashi K, Kakita A, et al. Neuropathology with clinical correlations of sporadic amyotrophic lateral sclerosis: 102 autopsy cases examined between 1962 and 2000. Brain Pathol 2003;13:10–22.
10. Ou SH, Wu F, Harrich D, et al. Cloning and characterization of a novel cellular protein, TDP-43, that binds to human immunodeficiency virus type 1 TAR DNA sequence motifs. J Virol 1995;69:3584–3596.
11. Buratti E, Dork T, Zuccato E, et al. Nuclear factor TDP-43 and SR proteins promote in vitro and in vivo CFTR exon 9 skipping. EMBO J 2001;20:1774–1784.
12. Neumann M, Sampathu DM, Kwong LK, et al. Ubiquitinated TDP-43 in frontotemporal lobar degeneration and amyotrophic lateral sclerosis. Science 2006;314:130–133.
13. Arai T, Hasegawa M, Akiyama H, et al. TDP-43 is a component of ubiquitin-positive tau-negative inclusions in frontotemporal lobar degeneration and amyotrophic lateral sclerosis. Biochem Biophys Res Commun 2006;351:602–611.
14. Davidson Y, Kelley T, Mackenzie IRA, et al. Ubiquitinated pathological lesions in frontotemporal lobar degeneration contain the TAR DNA-binding protein, TDP-43. Acta Neuropathol (Berl) 2007;113:521–533.
15. Wang H-Y, Wang I-F, Bose J, Shen C-KJ. Structural diversity and functional implications of the eukaryotic TDP gene family. Genomics 2004;130–139.
16. Buratti E, Brindisi A, Giombi M, et al. TDP-43 binds heterogeneous nuclear ribonucleoprotein A/B through its C-terminal tail. J Biol Chem 2005;280:37572–37584.
17. McKhann GM, Albert MS, Grossman M, et al. Clinical and pathological diagnosis of frontotemporal dementia: report of the work group on frontotemporal dementia and Pick's disease. Arch Neurol 2001;58:1803–1809.
18. Dickson DW, Josephs KA, Amador-Ortiz C. TDP-43 in differential diagnosis of motor neuron disorders. Acta Neuropathol (Berl) 2007;114:71–79.
19. Newell KL, Hyman BT, Growdon JH, Hedley-Whyte ET. Application of the National Institute on Aging (NIA)-Reagan Institute criteria for the neuropathological diagnosis of Alzheimer disease. J Neuropathol Exp Neurol 1999;58:1147–1155.
20. Kitagawa T, Aikawa T. Enzyme coupled immunoassay of insulin using a novel coupling reagent. J Biochem (Tokyo) 1976; 79:233–236.
21. Mori H, Kondo J, Ihara Y. Ubiquitin is a component of paired helical filaments in Alzheimer's disease. Science 1987;235: 1641–1644.
22. Arima K, Mizutani T, Alim MA, et al. NACP/alpha-synuclein and tau constitute two distinctive subsets of filaments in the same neuronal inclusions in brains from a family of parkinsonism and dementia with Lewy bodies: double-immunolabeling fluorescence and electron microscopic studies. Acta Neuropathol (Berl) 2000;100:115–121.
23. Hasegawa M, Arai T, Akiyama H, et al. TDP-43 is deposited in the Guam parkinsonism-dementia complex brains. Brain 2007;130:1386–1394.
24. Cairns NJ, Bigio EH, Mackenzie IR, et al. Neuropathologic diagnostic and nosologic criteria for frontotemporal lobar degeneration: consensus of the Consortium for Frontotemporal Lobar Degeneration. Acta Neuropathol (Berl) 2007;114:5–22.
25. Snowden J, Neary D, Mann D. Frontotemporal lobar degeneration: clinical and pathological relationships. Acta Neuropathol (Berl) 2007;114:31–38.
26. Amador-Ortiz C, Lin WL, Ahmed Z, et al. TDP-43 immunoreactivity in hippocampal sclerosis and Alzheimer's disease. Ann Neurol 2007;61:435–445.
27. Hasegawa M, Jakes R, Crowther RA, et al. Characterization of mAb AP422, a novel phosphorylation-dependent monoclonal antibody against tau protein. FEBS Lett 1996;384:25–30.
28. Fujiwara H, Hasegawa M, Dohmae N, et al. α-Synuclein is phosphorylated in synucleinopathy lesions. Nat Cell Biol 2002; 4:160–164.
29. Goedert M, Spillantini MG, Davies SW. Filamentous nerve cell inclusions in neurodegenerative diseases. Curr Opin Neurobiol 1998;8:619–632.
30. Goedert M. The significance of tau and alpha-synuclein inclusions in neurodegenerative diseases. Curr Opin Genet Dev 2001;11:343–351.
31. Sampathu DM, Neumann M, Kwong LK, et al. Pathological heterogeneity of frontotemporal lobar degeneration with ubiquitin-positive inclusions delineated by ubiquitin immunohistochemistry and novel monoclonal antibodies. Am J Pathol 2006;169:1343–1352.
32. Arai T, Ikeda K, Akiyama H, et al. Identification of amino-terminally cleaved tau fragments that distinguish progressive supranuclear palsy from corticobasal degeneration. Ann Neurol 2004;55:72–79.
33. Ishiguro K, Ohno H, Arai H, et al. Phosphorylated tau in human cerebrospinal fluid is a diagnostic marker for Alzheimer's disease. Neurosci Lett 1999;270:91–94.
34. Ishiguro K, Takamatsu M, Tomizawa K, et al. Tau protein kinase I converts normal tau protein into A68-like component of paired helical filaments. J Biol Chem 1992;267:10897–10901.
35. Baumann K, Mandelkow EM, Biernat J, et al. Abnormal Alzheimer-like phosphorylation of tau-protein by cyclin-dependent kinases cdk2 and cdk5. FEBS Lett 1993;336: 417–424.
36. Drewes G, Lichtenberg-Kraag B, Döring F, et al. Mitogen activated protein (MAP) kinase transforms tau protein into an Alzheimer-like state. EMBO J 1992;11:2131–2138.
37. Drewes G, Ebneth A, Preuss U, et al. MARK, a novel family of protein kinases that phosphorylate microtubule-associated proteins and trigger microtubule disruption. Cell 1997;89: 297–308.
38. Ishii A, Nonaka T, Taniguchi S, et al. Casein kinase 2 is the major enzyme in brain that phosphorylates Ser129 of human alpha-synuclein: implication for alpha-synucleinopathies. FEBS Lett 2007;581:4711–4717.
39. Arawaka S, Wada M, Goto S, et al. The role of G-protein-coupled receptor kinase 5 in pathogenesis of sporadic Parkinson's disease. J Neurosci 2006;26:9227–9238.
40. Pronin AN, Morris AJ, Surguchov A, Benovic JL. Synucleins are a novel class of substrates for G protein-coupled receptor kinases. J Biol Chem 2000;275:26515–26522.
41. Soret J, Tazi J. Phosphorylation-dependent control of the pre-mRNA splicing machinery. Prog Mol Subcell Biol 2003;31: 89–126.
42. Gross SD, Loijens JC, Anderson RA. The casein kinase Ialpha isoform is both physically positioned and functionally competent to regulate multiple events of mRNA metabolism. J Cell Sci 1999;112:2647–2656.
43. Mayrand SH, Dwen P, Pederson T. Serine/threonine phosphorylation regulates binding of C hnRNP proteins to pre-mRNA. Proc Natl Acad Sci USA 1993;90:7764–7768.
44. Habelhah H, Shah K, Huang L, et al. ERK phosphorylation drives cytoplasmic accumulation of hnRNP-K and inhibition of mRNA translation. Nat Cell Biol 2001;3:325–330.
45. van der Houven van Oordt W, Diaz-Meco MT, Lozano J, et al. The MKK(3/6)-p38-signaling cascade alters the subcellular distribution of hnRNP A1 and modulates alternative splicing regulation. J Cell Biol 2000;149:307–316.
46. Olsen JV, Blagoev B, Gnad F, et al. Global, in vivo, and site-specific phosphorylation dynamics in signaling networks. Cell 2006;127:635–648.

Human Molecular Genetics, 2009, Vol. 18, No. 18 **3353–3364**
doi:10.1093/hmg/ddp275
Advance Access published on June 10, 2009

Truncation and pathogenic mutations facilitate the formation of intracellular aggregates of TDP-43

Takashi Nonaka[1,*], Fuyuki Kametani[1], Tetsuaki Arai[2], Haruhiko Akiyama[2] and Masato Hasegawa[1,*]

[1]Department of Molecular Neurobiology and [2]Department of Psychogeriatrics, Tokyo Institute of Psychiatry, Tokyo Metropolitan Organization for Medical Research, 2-1-8 Kamikitazawa, Setagaya-ku, Tokyo 156-8585, Japan

Received April 5, 2009; Revised May 27, 2009; Accepted June 8, 2009

TAR DNA binding protein of 43 kDa (TDP-43) is a major component of the ubiquitin-positive inclusions found in the brain of patients with frontotemporal lobar degeneration (FTLD-U) and amyotrophic lateral sclerosis (ALS). Here, we report that expression of TDP-43 C-terminal fragments as green fluorescent protein (GFP) fusions in SH-SY5Y cells results in the formation of abnormally phosphorylated and ubiquitinated inclusions that are similar to those found in FTLD-U and ALS. Co-expression of DsRed-tagged full-length TDP-43 with GFP-tagged C-terminal fragments of TDP-43 causes formation of cytoplasmic inclusions positive for both GFP and DsRed. Cells with GFP and DsRed positive inclusions lack normal nuclear staining for endogenous TDP-43. These results suggest that GFP-tagged C-terminal fragments of TDP-43 are bound not only to transfected DsRed-full-length TDP-43 but also to endogenous TDP-43. Endogenous TDP-43 may be recruited to cytoplasmic aggregates of TDP-43 C-terminal fragments, which results in the failure of its nuclear localization and function. Interestingly, expression of GFP-tagged TDP-43 C-terminal fragments harboring pathogenic mutations that cause ALS significantly enhances the formation of inclusions. We also identified cleavage sites of TDP-43 C-terminal fragments deposited in the FTLD-U brains using mass spectrometric analyses. We propose that generation and aggregation of phosphorylated C-terminal fragments of TDP-43 play a primary role in the formation of inclusions and resultant loss of normal TDP-43 localization, leading to neuronal degeneration in TDP-43 proteinopathy.

INTRODUCTION

Progressive neuronal loss and abnormal protein deposits as intracellular inclusions are neuropathological features of the majority of neurodegenerative disorders, as exemplified by tau in Alzheimer's disease (AD), alpha-synuclein in Parkinson's disease (PD) and expanded polyglutamine gene products in CAG repeat diseases. Conformational changes, post-translational modifications or subcellular mislocalization of these normally highly soluble proteins results in the formation of abnormal protein aggregates or inclusions. It is important to establish the molecular mechanisms through which these proteins are converted to abnormal aggregates in neurons or glial cells in order to understand the pathogenesis of these diseases and to develop evidence-based, fundamental therapies.

Frontotemporal lobar degeneration with ubiquitinated inclusions (FTLD-U) and amyotrophic lateral sclerosis (ALS) are well-known neurodegenerative disorders. FTLD is the second most common form of cortical dementia in the population below the age of 65 years (1). ALS is the most common of the motor neuron diseases, being characterized by progressive weakness and muscular wasting, resulting in death within a few years. Ubiquitin (Ub)-positive inclusions are found as a pathological hallmark in brains of FTLD-U and ALS patients, as well as in AD and PD, but the major component of these inclusions had remained unknown. TAR-DNA binding protein of 43 kDa (TDP-43) has been identified as a major protein component of Ub-positive inclusions in FTLD-U and ALS brains (2,3). In 2008, mutations in the TDP-43 gene were discovered in familial

*To whom correspondence should be addressed. Tel: +81 333045701; Fax: +81 333298035; Email: nonakat@prit.go.jp (T.N.)/masato@prit.go.jp (M.H.)

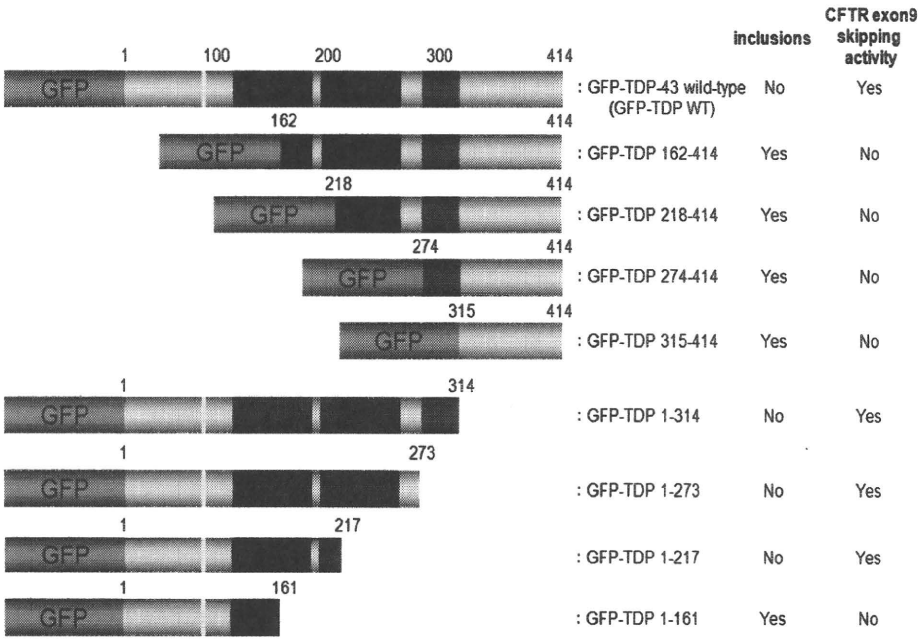

Figure 1. Schematic diagram of GFP-tagged N-terminal and C-terminal TDP-43 fragments. Green fluorescent protein (GFP), nuclear localization signal (NLS: 82–98 residues), two RNA-recognition motifs (RRM-1, 105–169 residues; RRM-2, 193–257 residues) and glycine-rich domain (274–314 residues) were colored green, yellow, blue and red, respectively. The formation of inclusions and the exon skipping ability of each fragment were reported on the right. The CFTR exon 9 skipping activity of these fragments were determined as shown in Fig. 5.

and sporadic cases of ALS (4–8), clearly indicating that abnormality of TDP-43 protein causes neurodegeneration. Very recently, it was also reported that two TDP-43 mutations were found in FTLD-MND patients (9). In previous genetic studies of familial ALS, superoxide dismutase 1 (SOD1) gene mutation was considered to be responsible for ~20% of cases (10,11). It has been reported, however, that TDP-43 is not deposited in spinal cords of familial ALS patients with SOD1 mutations (12,13). These observations suggest that the mechanisms of motor neuron degeneration caused by SOD1 mutations are different from those in sporadic ALS. TDP-43 is also a major component of skein-like inclusions seen in 100% of sporadic ALS cases (14). Thus, it is important to investigate the molecular mechanisms of TDP-43-mediated neurodegeneration in order to understand the pathogenesis and to develop effective treatments for sporadic ALS and other TDP-43 proteinopathies. One of the known biochemical features of TDP-43 deposited in FTLD-U and ALS brains is the presence of truncated TDP-43 fragments (2,3). Recently, using multiple anti-phosphorylated TDP-43 specific antibodies including pS409/410-specific antibodies, we have shown that 18–26 kDa C-terminal fragments of TDP-43 are major constituents of inclusions in FTLD-U and ALS brains (15).

In this study, we investigated the roles of fragmentation and pathogenic mutations of TDP-43 for the formation of Ub-positive inclusions in SH-SY5Y cells. Here we show that expression of TDP-43 C-terminal fragments results in the formation of cytoplasmic inclusions positive for antibodies to phosphorylated TDP-43 and Ub, and incorporation of newly synthesized endogenous full-length TDP-43 into cytoplasmic aggregates of the C-terminal fragments. Expression of fourteen pathogenic ALS mutations so far discovered in the TDP-43 gene shows a propensity to promote intracellular aggregation. Furthermore, using mass spectrometric analysis, we have successfully identified new cleavage sites of C-terminal fragments of TDP-43 deposited in FTLD-U brains.

RESULTS

Expression of TDP-43 fragments in SH-SY5Y cells

To examine whether C-terminal fragments of TDP-43 readily aggregate in neuronal cells, we expressed several kinds of N-terminal and C-terminal fragments of TDP-43 and full-length TDP-43 as GFP-fusions (Fig. 1). Confocal microscopic analysis showed that the fluorescence of GFP-tagged full-length TDP-43 (GFP-TDP WT) was mainly localized in the nuclei (Fig. 2B). This is consistent with the expression pattern of non-tagged wild-type TDP-43 (16), suggesting that the GFP tag did not alter the cellular localization of TDP-43.

When cells were transfected with GFP-TDP 162-414 or GFP-TDP 218-414, round or dot-like cytoplasmic structures with intense GFP fluorescence were found (Fig. 2C–F). These structures were positive for both anti-pS409/410 and anti-Ub antibodies (Fig. 2C–F). Cells expressing GFP-TDP 274–414 (Fig. 2G and H) and GFP-TDP 315–414 (Fig. 2I and J), on the other hand, showed diffuse GFP staining and pS409/410-positive but Ub-negative inclusion-like structures. We previously reported the presence of such pS409/410-positive and Ub-negative inclusions in the brains of FTLD-U and ALS cases (15). The expression of these all C-terminal fragments was found in cytoplasm by analyses using confocal microscopy (Fig. 2) and biochemical fractionation (Supplementary Material, Fig. S1A), because they lacks nuclear localization signal (16,17). Taken together, these results indicate that cytoplasmic expression of C-terminal

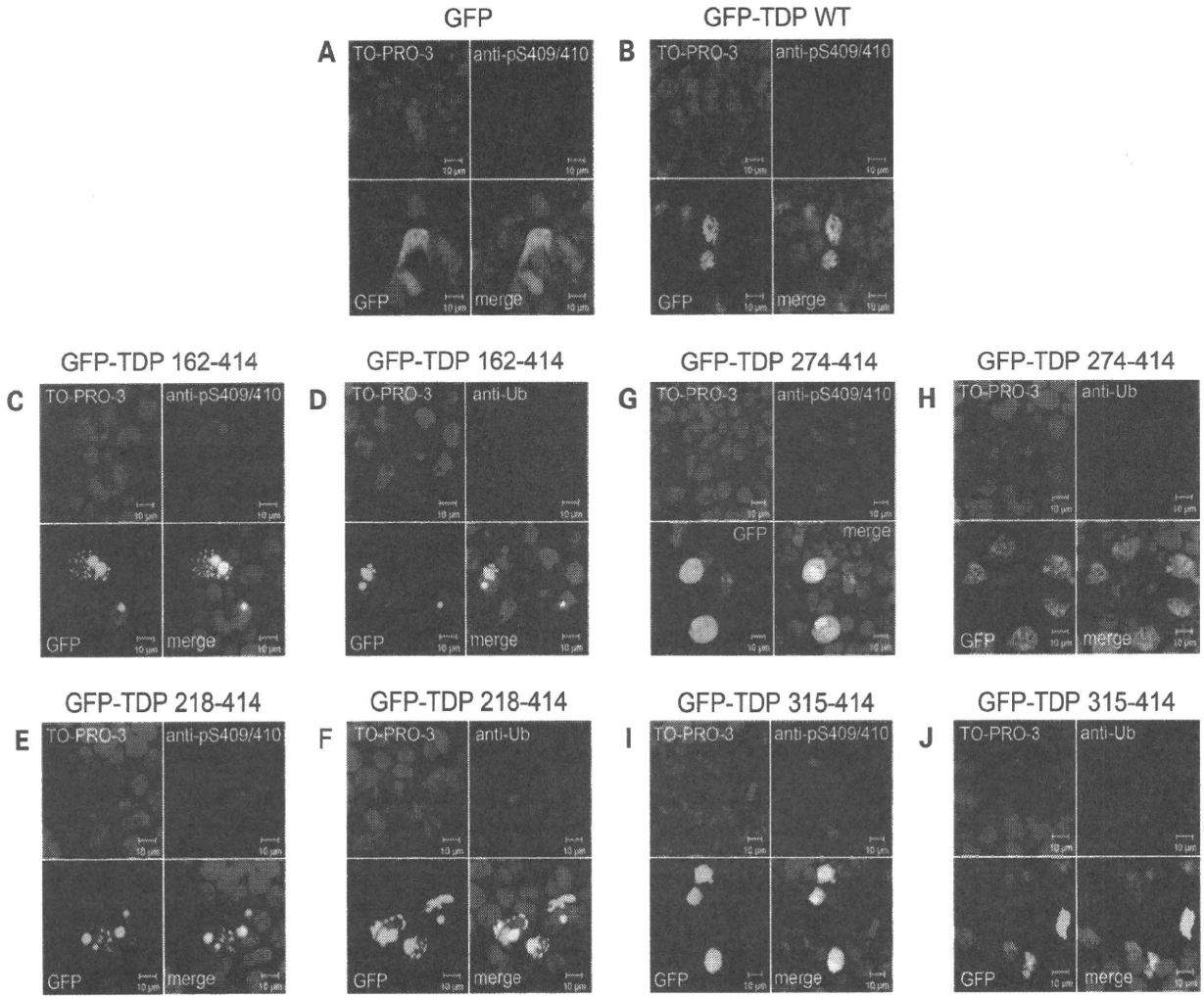

Figure 2. Expression of GFP-tagged C-terminal fragments of TDP-43 leads to aggregate formation in SH-SY5Y cells. SH-SY5Y cells 72 h post-transfection with GFP (**A**), GFP-tagged TDP-43 wild-type (GFP-TDP WT) (**B**), GFP-tagged fragments of residues 162–414 (GFP-TDP 162–414) (**C** and **D**), GFP-TDP 218–414 (**E** and **F**), GFP-TDP 274–414 (**G** and **H**) and GFP-TDP 315–414 (**I** and **J**) were stained with anti-pS409/410 (A, B, C, E, G, I) or anti-Ub (D, F, H, J). DNA was labeled with TO-PRO-3. Note that there are intracellular inclusion-like structures positive for both anti-Ub and anti-pS409/410 antibodies in cells expressing GFP-TDP 162–414 (C, D) and GFP-TDP 218–414 (E, F).

fragments of TDP-43 results in the formation of intracellular aggregates similar to those found in diseased brains.

N-terminal fragments of GFP-TDP-43 were also expressed in SH-SY5Y cells and analyzed using confocal microscopy and biochemical fractionation. As shown in Fig. 3A, irregularly shaped cytoplasmic structures with strong GFP fluorescence, which are partially positive for Ub, were observed in cells expressing GFP-TDP 1–161. Only a few aggregates positive for Ub were observed in cells transfected with GFP-TDP 1–217 (Fig. 3B). Since these fragments lack the epitope for anti-pS409/410, the phosphorylation state of these structures could not be determined by immunohistochemistry. None of the cells transfected with other N-terminal fragments had any Ub-positive inclusion-like structures (Fig. 3C and D). The results of biochemical fractionation showed that the amount of these N-terminal fragments was greater in the cytoplasm than in the nucleus, while that of GFP-TDP WT was greater in the nucleus than in the cytoplasm (Supplementary Material, Fig. S1A). These results suggest that truncations of TDP-43 C-terminal regions affect normal targeting of TDP-43 to nuclei. This observation is in good agreement with the previous report by Ayala *et al.* (18).

Since intracellular inclusion-like structures showed the highest-intensity GFP signals in Figs 2 and 3, they were able to be selectively detected by reducing the laser power at 488 nm. Quantitative analyses under such analytical conditions clearly indicated that significantly a larger number of intracellular aggregates were formed in cells expressing GFP-TDP 162–414, GFP-TDP 218–414 and GFP-TDP 1–161 than in cells expressing GFP-TDP WT (Fig. 3E).

Figure 4 shows the results of immunoblot analyses of cell lysates using anti-GFP, a commercially available phosphorylation-independent anti-TDP-43 (ProteinTech), and anti-pS409/410 antibodies. Anti-TDP-43 detected endogenous TDP-43 at 43 kDa, exogenous full-length TDP-43, all N-terminal fragments and GFP-TDP 162–414, but did not GFP-TDP 218–414, 274–414 and 315–414 (Fig. 4A and D). These results suggest that the epitopes of this antibody are located in the N-terminal region between 1 and 217 residues. Anti-GFP antibody stained all the exogenous TDP-43

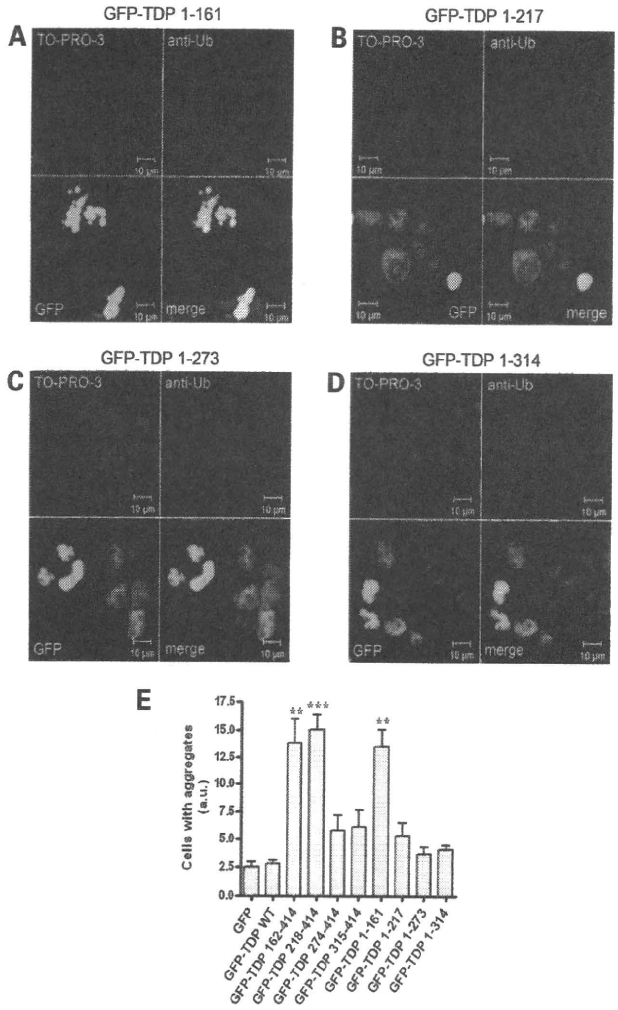

Figure 3. Expression of GFP-tagged N-terminal fragments of TDP-43 resulted in the formation of intracellular inclusions in SH-SY5Y cells. SH-SY5Y cells 72 h post-transfection with GFP-tagged fragments of 1–161 residues (GFP-TDP 1–161) (**A**), GFP-TDP 1–217 (**B**), GFP-TDP 1–273 (**C**) and GFP-TDP 1–314 (**D**) were stained with anti-Ub. DNA was labeled with TO-PRO-3. Note the characteristic inclusions detected with anti-Ub antibody in cells transfected with GFP-TDP 1–161. (**E**) The rates of cells including intracellular aggregates were calculated in arbitrary units. Fluorescence intensity within an area of ~800 × 800 μm was assessed by confocal microscopy. The intensity of GFP was calculated as a ratio to that of TO-PRO-3. Six areas per sample were measured ($n = 6$). Data are means ± SEM. $^{**}P < 0.01$; $^{***}P < 0.001$ by Student's *t*-test against the value of GFP-TDP WT.

(Fig. 4B and E). In these immunoblot analyses, we used the intensity of the bands of endogenous TDP-43 (arrows in Fig. 4A and D) as a loading control. While the amounts of exogenous protein are nearly constant, that of 1–161 is relatively low and those of 274–414 and 315–414 relatively high. Nevertheless, such variability does not affect the occurrence or absence of inclusion formation (Fig. 1). Endogenous and exogenous full-length TDP-43 (GFP-TDP WT) were detected mostly in TS-, TX- and Sar-soluble fractions, and were negative for anti-pS409/410 (Fig. 4).

Although GFP-TDP 162–414 was also detected in TS-, TX- and Sar-soluble fractions with anti-TDP-43 and anti-GFP, a slightly higher-molecular-weight band (~60 kDa, black arrowhead in Fig. 4C) was detected in Sar-soluble and insoluble fractions with anti-pS409/410. A similar band was only weakly detected with anti-TDP-43 (black arrowhead in Fig. 4A), and was negative to anti-GFP antibody. These results confirmed our previous reports that our anti-pS409/410 is specific to and is more sensitive in detecting abnormally accumulated TDP-43 than phosphorylation-independent antibodies such as anti-TDP-43 (ProteinTech) (15,16,19). Anti-GFP used here seems to be less sensitive in immunoblot. Anti-GFP may also be affected by possible structural changes during aggregates formation when applied to the Sarkosyl insoluble fraction. GFP-TDP 218–414 was mainly detected in Sar-soluble and -insoluble fractions with anti-GFP (Fig. 4B), and a slightly higher-molecular-weight band at 52 kDa (white arrowhead in Fig. 4C) and smears were visualized in the Sar-soluble and -insoluble fractions with anti-pS409/410. Similarly, pS409/410-positive bands were detected in the Sar-soluble and insoluble fractions of cell lysates expressing GFP-TDP 274–414 or GFP-TDP 315–414 (black-lined arrowhead for GFP-TDP-274–414; white-lined arrowhead for GFP-TDP 315–414 in Fig. 4C), although no abnormal band pattern was detected with anti-TDP-43 or anti-GFP.

The N-terminal fragments, including GFP-TDP 1–314, GFP-TDP 1–273 and GFP-TDP 1–217, were detected mainly in the TS- and TX-soluble fractions, together with GFP-TDP WT and endogenous TDP-43 (Fig. 4D and E). However, GFP-TDP 1–161, the shortest N-terminal fragment, was detected only in the Sar-soluble fraction (black-lined arrowheads in Fig. 4D and E), which is consistent with the inclusion formation observed in cells expressing this fragment, as shown in Fig. 3A.

Loss of function and intracellular accumulation of TDP-43 fragments

TDP-43 has been reported to regulate the alternative splicing of exon 9 of cystic fibrosis transmembrane conductance regulator (CFTR) transcripts (20). TDP-43 is capable of binding to a (UG)nUm element in CFTR intron 8 near its junction with exon 9. Through this binding, TDP-43 enhances the exon skipping of exon 9 during CFTR splicing. To evaluate the functional significance of TDP-43 fragments used in this study, we performed CFTR exon 9 skipping assay (16). We co-transfected the expression plasmid of TDP-43 wild-type or fragments with the reporter plasmid pSPL3-CFTR9 (including a TG11T7 polymorphic locus) (16) into SH-SY5Y cells. The transcripts with and without the CFTR exon 9 insert are expected to be 360 and 177 bp long, respectively (16), and these were analyzed by RT–PCR. As shown in Fig. 5, mRNA from cells transfected with empty vector pEGFP gave only one RT–PCR band of 360 bp, while that from cells transfected with TDP-43 wild-type gave two RT–PCR bands, 360 and 177 bp, showing that skipping of CFTR exon 9 was increased by expression of GFP-TDP WT. We also confirmed that the GFP portion did not affect the CFTR exon skipping activity of TDP-43. All mRNAs from cells co-transfected with the C-terminal fragments showed one RT–PCR band of 360 bp (Fig. 5A). Of the four mRNAs from cells co-transfected with the N-terminal fragments, mRNA from GFP-TDP 1-161 showed a band of 360 bp, while the others showed two bands of 360 and 177 bp (Fig. 5B). These results indicate that the fragments without

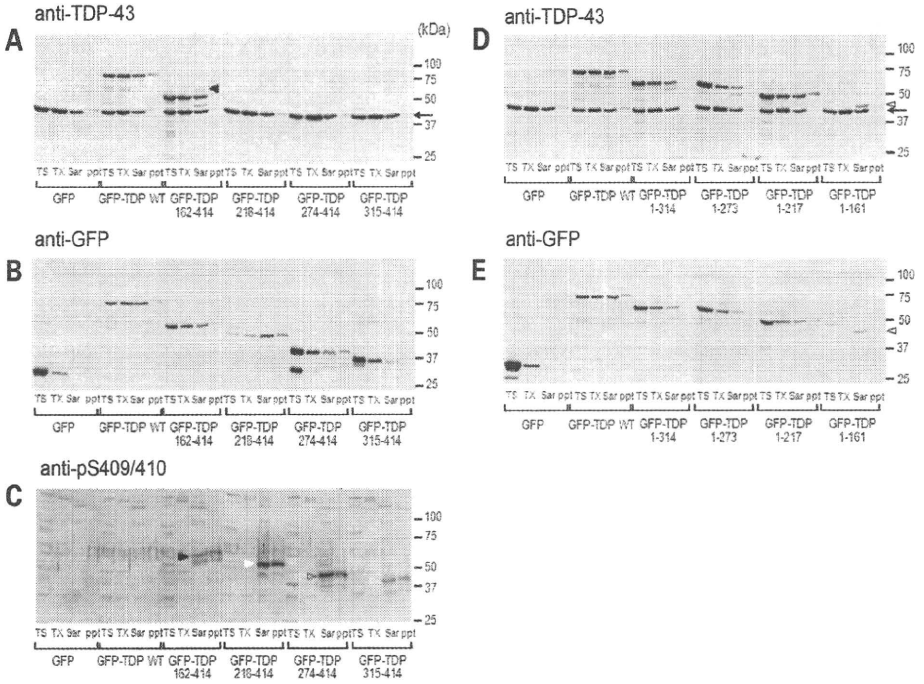

Figure 4. Immunoblot analyses of inclusions composed of GFP-tagged N-terminal and C-terminal fragments of TDP-43. SH-SY5Y cells, 72 h post-transfection with GFP alone or GFP-fused TDP-43 fragments, were sequentially extracted with Tris-saline (TS), 1% Triton X-100 (TX) and 1% Sarkosyl (Sar), and the supernatants and the Sarkosyl-insoluble pellets (ppt) were subjected to SDS–PAGE. Bands were transferred to PVDF membrane and probed with anti-TDP-43 antibody (**A** and **D**), anti-GFP antibody (**B** and **E**) and anti-pS409/410 antibody (**C**). The arrow indicated the band of endogenous TDP-43. Note that bands of pS409/410-positive C-terminal fragments were detected in Sarkosyl-soluble or -insoluble fractions of cells expressing GFP-TDP 162–414 (black arrowhead in C), GFP-TDP 218–414 (white arrowhead in C), GFP-TDP 274–414 (black-lined arrowhead in C) and GFP-TDP 315–414 (white-lined arrowhead in C), and that N-terminal fragment of GFP-TDP 1–161 was recovered in TX-insoluble fractions (black-lined arrowhead in D and E).

the entire RRM-1 motif do not have exon skipping activity, while the wild-type and fragments with the RRM-1 motif have the activity (Figs 1 and 5). These results are in good agreement with the observation by Buratti and Baralle (21) that the RRM-1 domain is necessary for binding with RNA. It is noteworthy that all the TDP-43 fragments which form intracellular aggregates lack exon skipping activity.

Expression of TDP-43 C-terminal fragment facilitates aggregation of full-length TDP-43 in SH-SY5Y cells

To test whether C-terminal fragments of TDP-43 interact with full-length TDP-43, C-terminal fragments of GFP-TDP-43 or full-length GFP-TDP-43 was co-expressed with full-length DsRed-fused TDP-43 (DsRed-TDP-43) in SH-SY5Y cells. Immunoprecipitation experiments of cell lysates using agarose conjugated anti-GFP followed by immunoblotting with anti-RFP or anti-TDP-43 showed that GFP-TDP-43 C-terminal fragments as well as full-length GFP-TDP-43 were bound to full-length DsRed-TDP-43 (Fig. 6). Full-length GFP-TDP-43 was found to more strongly interact with DsRed-TDP-43 than any other C-terminal fragments of GFP-TDP-43. The experiments also showed a weak but notable interaction between endogenous TDP-43 and full-length GFP-TDP-43 or C-terminal fragments of GFP-TDP-43. These results suggest that both full-length GFP-TDP-43 and its C-terminal fragments interact not only with full-length DsRed-TDP-43 but also with endogenous TDP-43 in SH-SY5Y cells.

To monitor the intracellular interaction between endogenous TDP-43 and C-terminal fragments of GFP-TDP-43, SH-SY5Y cells were transfected with GFP-TDP 162–414 or GFP-TDP 218–414 and analyzed by confocal microscopy. Immunostaining using anti-TDP-43 showed that full-length GFP-TDP-43 was co-localized with endogenous TDP-43 in nuclei (Fig. 7A). We observed that GFP signals from cytoplasmic inclusions of GFP-TDP 162–414 or GFP-TDP 218–414 were overlapped with immunoreactivities of anti-TDP-43. Furthermore, immunoreactivities of anti-TDP-43 were almost eliminated from the nuclei of these cells (Fig. 7B and C). When full-length GFP-TDP-43 was co-expressed with full-length DsRed-TDP-43, both proteins were found to be localized in nuclei with no formation of inclusion-like structures (Fig. 7D). In contrast, round cytoplasmic inclusions with both GFP and DsRed signals appeared when GFP-TDP 162–414 (Fig. 7E) or GFP-TDP 218–414 (Fig. 7F) was co-expressed with full-length DsRed-TDP-43. These results indicate that endogenous TDP-43 or exogenous full-length DsRed-TDP-43 is trapped into cytoplasmic inclusions formed by GFP-TDP 162–414 or GFP-TDP 218–414, which is consistent with the results of immunoprecipitation experiments shown in Fig. 6.

Effects of pathogenic mutations on aggregation of TDP-43

Then, we tested the effect of mutations of the TDP-43 gene found in familial and sporadic ALS cases on the intracellular aggregates of C-terminal fragments of GFP-TDP-43 (GFP-TDP 162–414). GFP-TDP 162–414 with or without mutations was expressed in SH-SY5Y cells, which were then analyzed by immunoblot and confocal microscopy. We first confirmed almost same expression levels of all exogenous